HETEROCYCLES, Vol. 89, No. 3, 2014, pp. 579 - 625. © 2014 The Japan Institute of Heterocyclic Chemistry
Received, 12th November, 2013, Accepted, 28th November, 2013, Published online, 17th December, 2013
DOI: 10.3987/REV-13-787

PHOTOINDUCED ELECTRON TRANSFER-INITIATED CYCLIZATION REACTIONS AND ASYMMETRIC TRANSFORMATIONS OF (*Z*)-α-DEHYDROAMINO ACID DERIVATIVES

Tetsutaro Igarashi and Tadamitsu Sakurai*

Department of Material and Life Chemistry, Faculty of Engineering, Kanagawa University, Kanagawa-ku, Yokohama 221-8686, Japan

Abstract – We systematically investigated the cyclization reactions of *N*-acyl-α-dehydroamino acid derivatives, initiated by electron transfer (ET) from aliphatic amines to these derivatives in the excited state. On the basis of the percent conversion of the starting α-dehydroamino acid and the composition of the cyclization products, we demonstrated that the photoinduced ET reactions of *N*-acyl-α-dehydroarylalaninamides, 1,2,4-triazole-substituted α-dehydro-arylalaninamides, and *N*-acyl-α-dehydroarylalanine alkyl esters efficiently proceeded to afford various 3,4-dihydroquinolinone; quinolinone; and 4,5-dihydrooxazole derivatives, respectively, with high selectivities. In addition, the introduction of chiral auxiliary groups into *N*-acyl-α-dehydroamino acid amide and ester derivatives and the presence of chiral aliphatic amines induced efficient diastereoselective and enantioselective photocyclization reactions of these amide and ester derivatives, respectively, to enable the construction of the chiral dihydroquinolinone and dihydrooxazole rings.

CONTENTS

1. INTRODUCTION

Organic photochemical reactions contribute to unique methods for the synthesis of organic compounds with complicated structures, which could not be synthesized by conventional methods.[1,2] Particularly, photocycloaddition and photocyclization reactions have enabled the construction of various types of carbocyclic and heterocyclic ring systems, even at low temperatures. Recently, photoinduced electron transfer (PET)-initiated cyclization reactions have received considerable attention owing to their wide range of synthetic applications.[1a,2] In addition, a systematic study of these PET reactions proceeding through exciplexes or radical ions has provided new and interesting mechanistic information on organic photochemistry. Whether one should employ one-electron reductants or one-electron oxidants in these PET reactions depends on the redox potentials of the reactants that undergo PET-initiated cycloaddition and cyclization.

It has long been known that the irradiation of various types of aromatic olefins, including heteroaromatic-substituted olefins, induces interesting cycloaddition and cyclization reactions in the presence of oxidizing agents to produce valuable carbocyclic and heterocyclic compounds.[1b,c] However, there has been no systematic study on the photochemical reactivity of naturally occurring α,β-unsaturated aromatic amino acid derivatives (aromatic α-dehydroamino acid derivatives) that have potential pharmacological activity. Because these dehydroamino acids possess photochemically reactive olefins, they are expected to undergo either photocycloaddition or photocyclization under various irradiation conditions to construct pharmacologically active heterocyclic rings. Unfortunately, the high thermal reactivity of unsubstituted α-dehydroamino acids renders the use of these amino acids as reactants very difficult for the photochemical study.[3] To overcome this difficulty, the amino functional group of α-dehydroamino acids was *N*-acylated to enable the design of *N*-acyl-α-dehydroarylalaninamides and *N*-acyl-α-dehydroarylalanine alkyl esters. We expected that the presence of the acylamino- and aryl-substituted vinyl groups in these α-dehydroamino acid derivatives would enhance the ability to remove an electron from typical one-electron reductants. In this review, we describe intramolecular and intermolecular PET-initiated cyclization reactions of various substituted α-dehydroamino acid derivatives and PET-initiated diastereoselective and enantioselective cyclization reactions of these derivatives.

2. PHOTOINDUCED ELECTRON TRANSFER-INITIATED CYCLIZATION REACTIONS

2-1. (*Z*)-*N*-Acyl-α-dehydro(1-naphthyl)alanine *N*′-dialkylaminopropylamides[4–7]

In previous studies, we have shown that the selective excitation of the 1-naphthyl chromophore in *N*-acetyl-1-naphthylalanine *N*′-diethylaminopropylamide **1** causes efficient fluorescence quenching of this chromophore.[8] The effects of solvent polarity, solvent viscosity, and the distance between the naphthalene ring and diethylamino nitrogen on the rate constant of the fluorescence quenching presented kinetic evidence for the participation of a singlet exciplex mechanism in both polar and nonpolar solvents. In addition, the observation of a correlation between the free energy change in electron transfer (ET) and the solvent viscosity supported the existence of an exciplex-derived solvent-separated radical ion pair intermediate in polar solvents (Scheme 1).

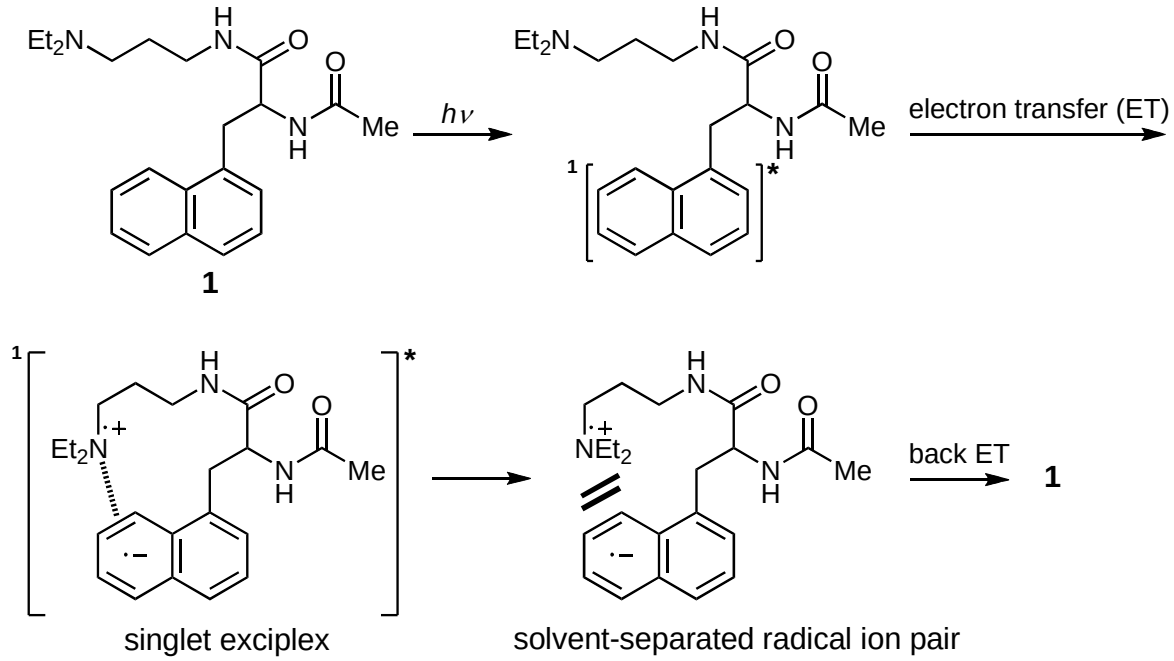

Scheme 1

Thus, it is expected that intramolecular PET in (*Z*)-*N*-acyl-α-dehydro(1-naphthyl)alanine *N*′-dialkylaminopropylamides (*Z*)-**2** generates the corresponding radical ion pair intermediates in polar solvents (Figure 1).

Substituted α-dehydro(1-naphthyl)alaninamides (*Z*)-**2** were synthesized by the ring-opening reactions of thermodynamically more stable (*Z*)-4-(1-naphthylmethylene)-5(4*H*)-oxazolones, prepared from the improved Perkin reaction between aromatic aldehydes and *N*-acyl glycines, with *N*,*N*-dialkylaminopropylamines in good yields (Scheme 2).[9] To test the photocyclization reaction,

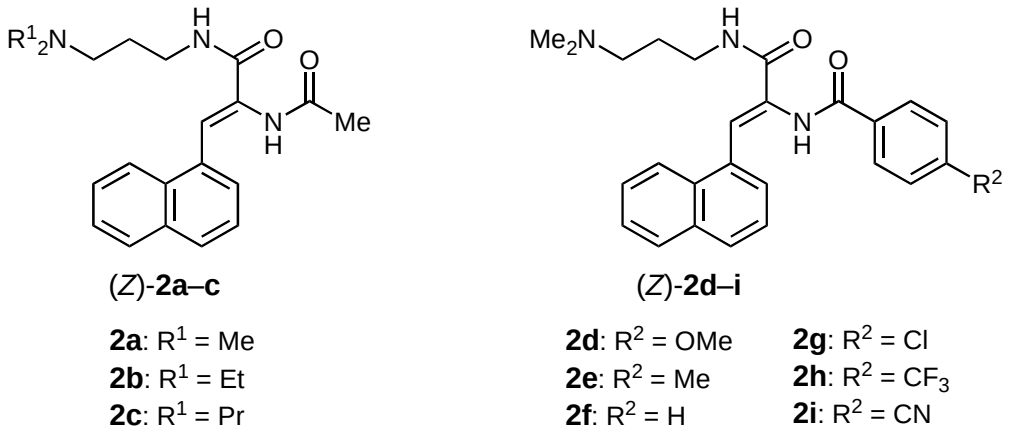

Figure 1. Structures of (*Z*)-**2a**–**i**

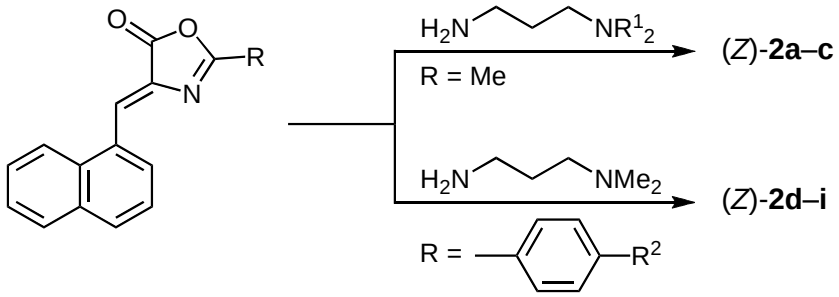

Scheme 2

a nitrogen-saturated methanol solution containing (*Z*)-**2a** was irradiated at room temperature. When the crystalline product mixture was washed with ether and hexane, analytical grade 3,4-dihydrobenzo[*f*]quinolinone **3a** was isolated in 60% yield. ^{1}H NMR spectral analysis of the remaining products indicated the formation of benzo[*f*]isoquinoline **4a**, *cis*-4,5-dihydrooxazole *cis*-**5a**, and (*E*)-**2a** (Scheme 3).

The photoproducts isolated were very stable during irradiation, which allowed us to monitor the reaction by ^{1}H NMR spectroscopy, as shown in Table 1. Time-course analysis of the product composition demonstrated the rapid production of (*E*)-**2a** and the subsequent increase in the percent compositions of **3a**–**5a** with a decrease in the percent compositions of (*Z*)- and (*E*)-**2a**; these results are consistent with a mechanism in which these excited-state isomers serve as precursors of the photoproducts **3a**–**5a**.

In addition to the observation of intramolecular fluorescence quenching by ET from the dimethylamino nitrogen to the excited-state naphthylmethylene moiety in **2a**, energy-minimized conformations for (*Z*)-**2a** and (*E*)-**2a** suggest that the (*E*)-**2a**-derived radical ion pair is the precursor of the dihydrobenzoquinolinone **3a** and the dihydrooxazole **5a** while the benzoisoquinoline **4a** is formed via

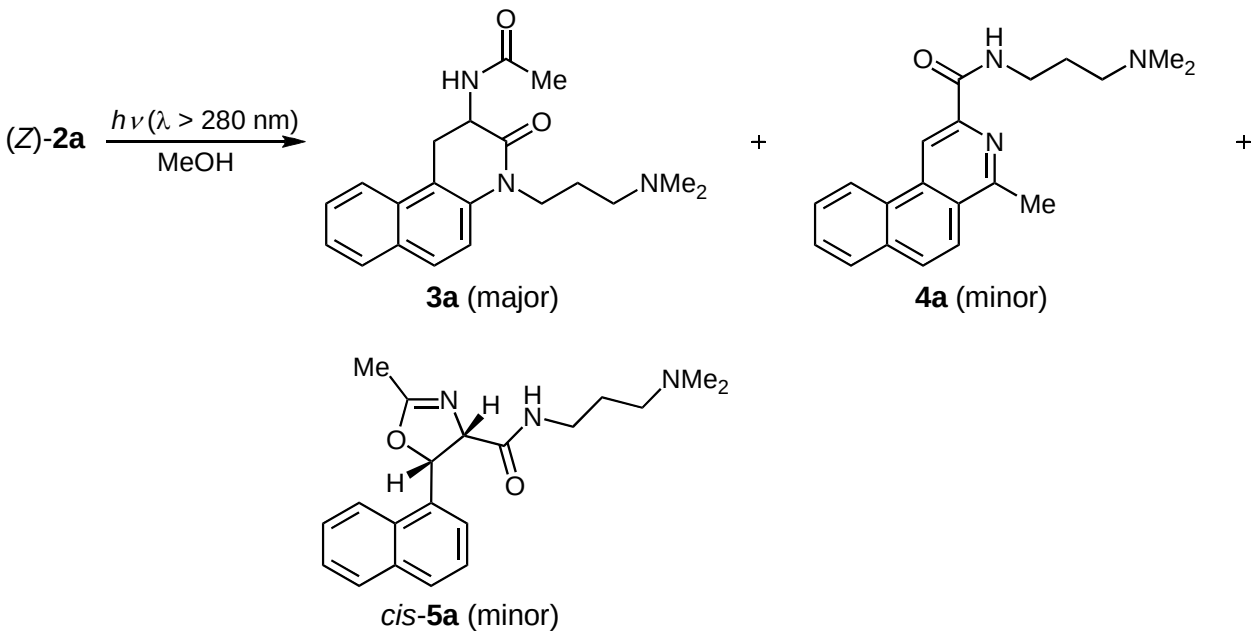

Scheme 3

Table 1. Relation between irradiation time and composition (%) of each compound obtained by the irradiation of (*Z*)-**2a** in MeOH

Compound	Irradiation time /min						
	0	15	30	45	60	90	120
(Z)-**2a**	100	39.0	27.4	18.7	11.8	3.2	0.0
(E)-**2a**	0	40.5	31.6	21.8	15.1	4.9	1.5
3a	0	14.8	31.6	46.4	58.9	74.9	78.5
4a	0	5.1	8.2	11.4	12.1	14.3	17.6
cis-**5a**	0	0.5	1.2	1.7	2.1	2.7	2.4

cyclization of the (*Z*)-**2a**-derived radical ion pair, as shown in Scheme 4.

To extend the synthetic utility of the highly selective cyclization reaction constructing the 3,4-dihydroquinolinone ring, the effects of the substituents R^1 and R^2 on the photoreactivity of **2a**–**c** and **2d**–**f**, respectively, and the selectivity of **3** were explored under the same irradiation conditions, as those for (*Z*)-**2a** (Table 2). Although R^1 in **2b** and **2c** exerts only a small effect on the photoreactivity (conversion) of **2a**, the electron-withdrawing Cl, CF_3, and CN groups in **2g**–**i** lower the photoreactivity of **2f**.

It is likely that the charge-transfer interaction between the dimethylamino and aromatic acyl groups

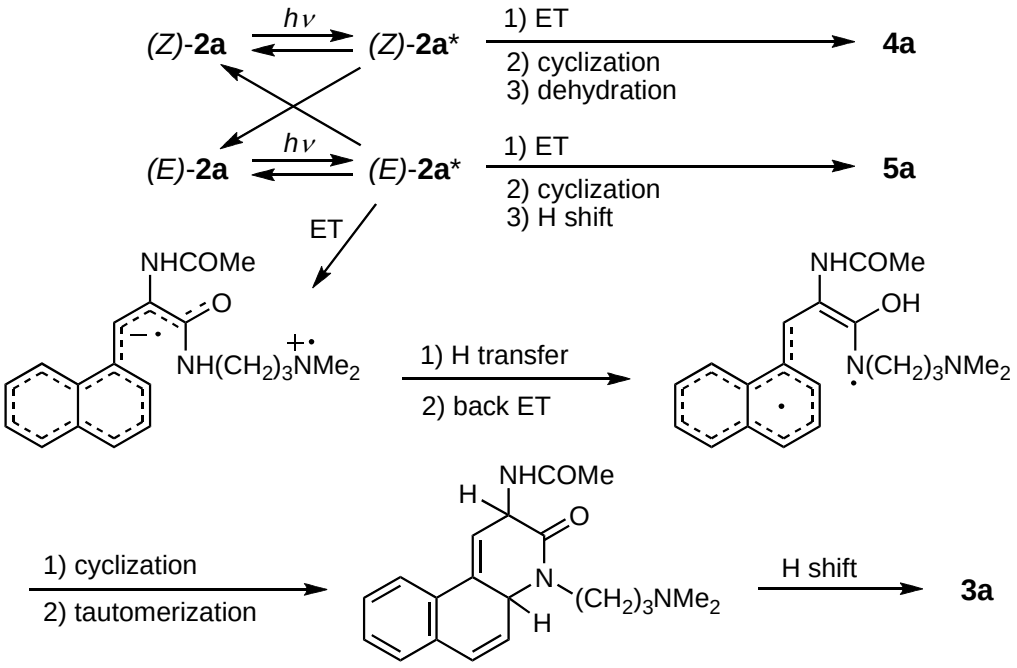

Scheme 4

Table 2. Substituent effects on the photoreactivity and product composition of the starting *(Z)*-**2** in MeOH

(*Z*)-**2** (R^1 or R^2)	Irradiation time (min)	Conversion (%)	Composition (%)				
			(Z)-**2**	*(E)*-**2**	**3**	**4**	**5**[a]
2a (R^1 = Me)	15	20.5	39.0	40.5	14.8	5.1	0.5
	120	98.5	0.0	1.5	78.5	17.6	2.4
2b (R^1 = Et)	15	17.3	46.8	36.0	14.6	2.0	0.7
	120	93.3	5.9	0.8	83.8	5.9	3.6
2c (R^1 = Pr)	15	23.1	39.6	37.3	20.5	2.0	0.6
	120	100.0	0.0	0.0	92.2	5.1	2.7
2d (R^2 = OMe)	15	21.6	55.6	22.8	19.2	1.4	1.0
	120	95.0	3.2	1.8	86.5	3.2	5.2
2e (R^2 = Me)	15	18.9	55.5	25.6	15.6	1.2	2.1
	120	96.5	2.2	1.3	86.2	2.2	8.1
2f (R^2 = H)	15	14.2	59.1	26.6	11.9	0.3	2.0
	120	95.9	2.0	2.1	84.5	1.4	10.0
2g (R^2 = Cl)	15	12.0	63.5	24.5	9.8	0.0	2.2
	120	75.7	15.6	8.7	64.1	0.7	10.9
2h (R^2 = CF_3)	15	3.2	81.1	15.7	2.1	0.0	1.1
	120	48.9	34.5	16.6	37.5	0.0	11.4
2i (R^2 = CN)	15	1.8	94.3	3.9	0.7	0.0	1.1
	120	11.3	71.1	17.6	5.9	0.0	5.4

[a] The sum of *cis*- and *trans*-isomer compositions.

contributes to the deactivation of the excited-state (*Z*)- and (*E*)-isomers. In contrast, the selectivity of the photochemically stable dihydrobenzoquinolinone derivatives **3a**–**i** (39–92%) is not significantly affected by the substituents R^1 and R^2. Thus, the intramolecular PET-initiated cyclization reactions described above constitute a novel photochemical method for constructing the 3,4-dihydrobenzo-quinolinone ring.

In the course of a study regarding the inhibitory effect of oxygen on the aforementioned photocyclization reactions, we found the quantitative conversion of (*Z*)-*N*-acetyl-α-dehydroarylalanine *N′*-dialkylaminoethylamides (*Z*)-**6a**–**d** to the corresponding (*Z*)-2-imidazolin-5-one derivatives (*Z*)-**7** and hydrogen peroxide in oxygen-saturated methanol (Scheme 5). The X-ray single-crystal structural analysis of the imidazolinone (*Z*)-**7c** provided definitive evidence for its structure and configuration (Scheme 5).

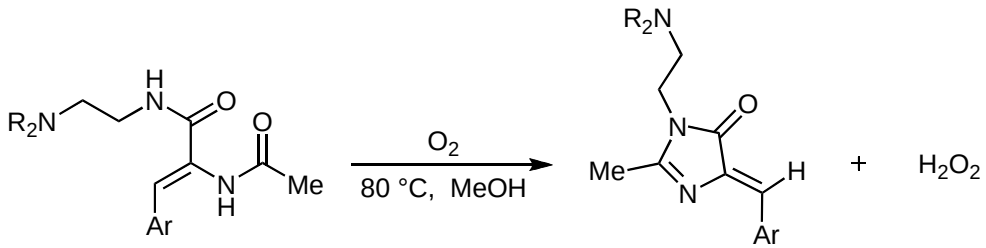

(*Z*)-**6a**–**d** (*Z*)-**7**

6a: Ar = 1-naphthyl, R = Me
6b: Ar = 1-naphthyl, R = Et
6c: Ar = phenyl, R = Me
6d: Ar = phenyl, R = Et

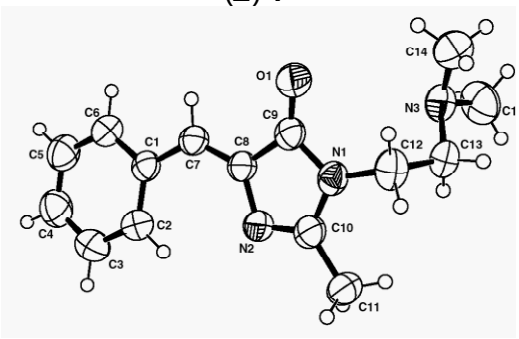

Crystal structure of (*Z*)-**7c**

Scheme 5

The facts that the protic polar solvent methanol greatly accelerates the cyclization reaction and the exclusion of a dimethylamino group in reactant (*Z*)-**6a** completely inhibits this reaction substantiate the participation of ET from the tertiary amino nitrogen to oxygen in the initiation step of the reaction, as shown in Scheme 6.

Although many routes to 2-imidazolin-5-one derivatives have been developed,[10] there is no synthetic method that utilizes the cyclization reaction of *N*-acetyl-α-dehydroarylalaninamides activated by ET to oxygen in methanol. Therefore, the oxidative cyclization reaction of (*Z*)-**6** provides a novel synthetic route to the imidazolinone (*Z*)-**7**.

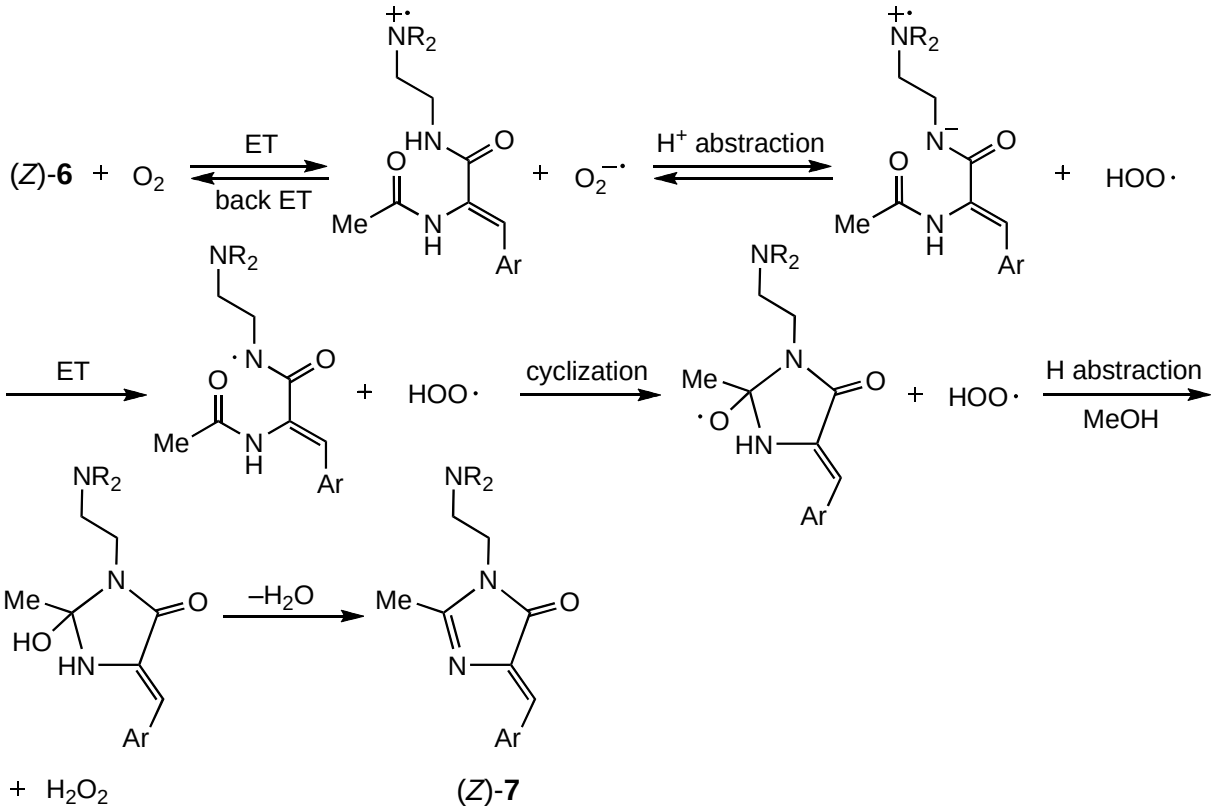

Scheme 6

2-2. (*Z*)-*N*-Acyl-α-dehydronaphthylalanine *N*′-alkylamides[11–13]

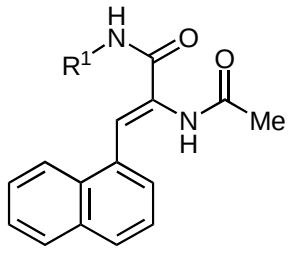

(*Z*)-**8a–g**

8a: R^1 = H, **8b**: R^1 = Me
8c: R^1 = Et, **8d**: R^1 = Pr
8e: R^1 = *i*-Pr, **8f**: R^1 = Bu
8g: R^1 = $PhCH_2$

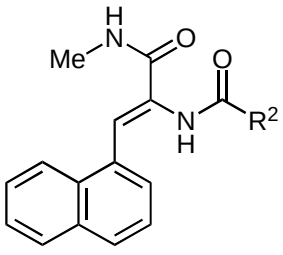

(*Z*)-**9a–f**

9a: R^2 = Ph
9b: R^2 = 4-$OMeC_6H_4$
9c: R^2 = 4-BrC_6H_4
9d: R^2 = 4-$CF_3C_6H_4$
9e: R^2 = 2,4-$(OMe)_2C_6H_3$
9f: R^2 = *t*-Bu

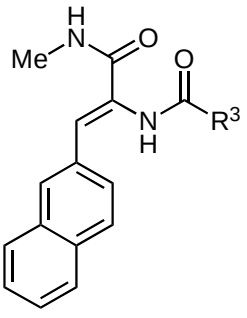

(*Z*)-**10a–c**

10a: R^3 = Ph
10b: R^3 = 4-$OMeC_6H_4$
10c: R^3 = 2,4-$(OMe)_2C_6H_3$

Figure 2. Structures of (*Z*)-**8a–g**, (*Z*)-**9a–f**, and (*Z*)-**10a–c**

To explore the PET-initiated cyclization reaction (enabling the construction of the dihydroquinolinone ring) in more detail, (*Z*)-*N*-acyl-α-dehydronaphthylalaninamides **8a**–**g**, **9a**–**f**, and **10a**–**c** were designed and synthesized in good yields according to the same procedures as described in the preceding section (Figure 2). Irradiation of a nitrogen-saturated methanol solution containing **8f** (R^1 = Bu) and triethylamine (TEA) (electron donor) at room temperature resulted in the formation of 3,4-dihydrobenzo[*f*]quinolinone **11f** (isolated yield, 45%), benzo[*f*]isoquinoline **12f** (14%), and (*E*)-**8f** (5%) (Scheme 7). ^{1}H NMR spectral analysis of the irradiated mixture suggested the existence of minor amounts of *cis*-4,5-dihydrooxazole **13f**.

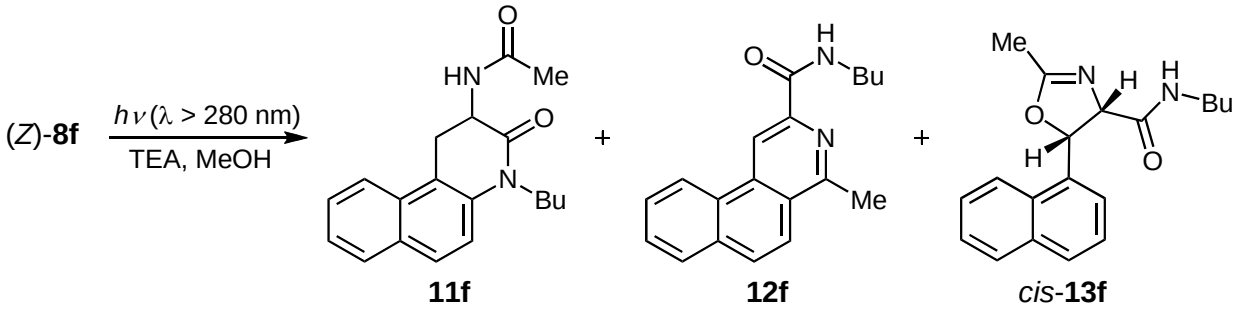

Scheme 7

The finding that the fluorescence of **8f** in methanol is quenched by TEA, according to the Stern–Volmer equation, is consistent with the involvement of ET from TEA to the excited-state **8f** in the primary step of the photocyclization reaction observed, as already suggested. Furthermore, ^{1}H NMR spectral analysis of the reaction showed no change in the TEA concentration during irradiation, and the *N′*-butylamide deuteron of the starting (*Z*)-**8f** was transferred to the 3-position on the dihydroquinolinone ring formed by its photocyclizaton. Thus, the intermolecular PET-initiated cyclization processes shown in Scheme 8 provide a reasonable explanation for these observations.

Comparison of the dependence of the product compositions, derived from (*Z*)-**8f** and (*E*)-**8f**, on irradiation time confirms that photoisomerization between these two isomers is not as fast as the subsequent ET and cyclization processes (Table 3). Additionally, analysis of the compositions for **11f**–**13f** led us to conclude that the excited-state (*Z*)- and (*E*)-isomers serve as precursors to benzoisoquinoline **12f** and dihydrobenzoquinolinone **11f**/dihydrooxazole **13f**, respectively, as depicted in Scheme 8. ET from TEA to the two excited-state isomers supports a mechanism in which the isoquinoline skeleton is constructed by the cyclization of the (*Z*)-isomer-derived radical anion.

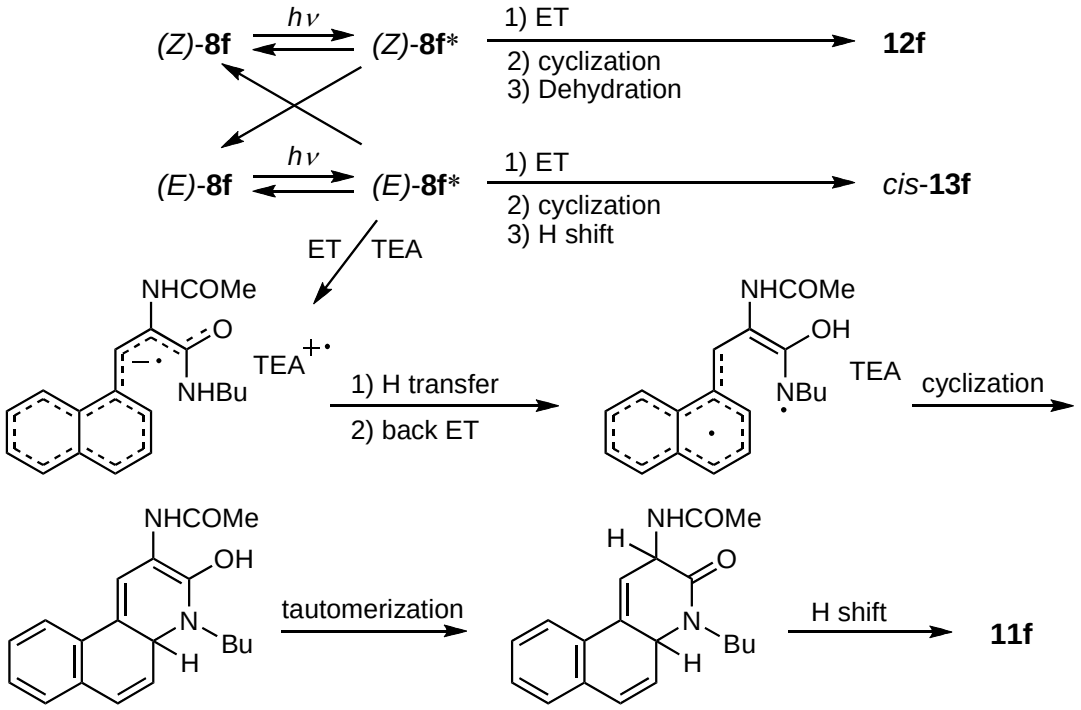

Scheme 8

Table 3. Relation between irradiation time and composition (%) of each compound obtained by the irradiation of (*Z*)-**8f** and (*E*)-**8f** in MeOH-TEA at room temperature

Compound	Irradiation time (h)			
	0	0.5	1.0	1.5
(Z)-**8f**	100 (0)	60.7 (26.9)	43.5 (30.6)	34.2 (27.4)
(E)-**8f**	0 (100)	31.6 (56.0)	38.0 (40.2)	35.8 (31.4)
11f	0 (0)	4.3 (15.8)	11.7 (25.8)	20.4 (35.4)
12f	0 (0)	3.2 (0.9)	6.5 (2.5)	9.0 (4.8)
cis-**13f**	0 (0)	0.1 (0.5)	0.3 (0.8)	0.6 (1.0)

To inspect the synthetic utility of the intermolecular PET-initiated cyclization reaction, effects of the substituent R^1 on the photoreactivity (conversion) of **8** and selectivity of **11**–**13** were analyzed (Table 4). Clearly, dihydrobenzoquinolinone **11** gives the highest selectivity among these three cyclization products, and its selectivity decreases with an increase in the steric bulk of R^1. This decrease in selectivity is reflected in enhanced selectivity for **12** and **13**, providing additional evidence for a mechanism in which ET to the excited-state (*E*)-**8** and the subsequent cyclization to **11** occurs in competition with the isomerization to (*Z*)-**8** and cyclization eventually affording **13**. It is also noteworthy that the

introduction of bulky *tert*-butyl and phenyl groups as R^1 completely inhibits the formation of the corresponding dihydrobenzoquinolinones.

Table 4. Substituent effects on the composition of each compound obtained by the 5 h irradiation of the starting *(Z)*-**8** in MeOH containing TEA at room temperature

(Z)-**8** (R^1)	Conversion (%)	Composition (%)					
		(Z)-**8**	*(E)*-**8**	**11**	**12**	*cis*-**13**	*trans*-**13**
8a (H)	94.4	2.2	3.4	76.3	13.0	5.2	0.0
8b (Me)	96.9	1.4	1.7	85.0	11.0	0.9	0.0
8c (Et)	91.0	4.1	4.9	74.5	14.9	1.5	0.0
8d (Pr)	87.0	5.7	7.3	68.4	17.4	1.2	0.0
8e (*i*-Pr)	76.9	8.9	14.2	43.3	26.2	5.8	1.5
8f (Bu)	90.4	4.0	5.6	69.0	19.6	1.8	0.0
8g ($PhCH_2$)	94.7	1.8	3.5	70.8	20.8	3.1	0.0

Meanwhile, when nitrogen-saturated methanol solutions containing (*Z*)-**9** or (*Z*)-**10** were irradiated in the presence of TEA (for **9**) or DBU (for **10**) under the same conditions as those for (*Z*)-**8**, the corresponding 3,4-dihydrobenzoquinolinones **14** (Scheme 9) or **16** (Scheme 10) were produced with high selectivity (>82% and >63%, respectively), along with minor amounts of 4,5-dihydrooxazoles **15** or **17**. Replacement of the *N*-acetyl group in **8** by bulky aroyl and pivaloyl groups greatly lowers the photoreactivity of this α-dehydro(1-naphthyl)alaninamide. As already suggested in the preceding section, this may be owing to the decreased efficiency of ET from TEA to the 1-naphthylmethylene moiety of **9** in the excited state. Moreover, substituting the 1-naphthylmethylene chromophore with 2-naphthylmethylene drastically lowered the reactivity of (*Z*)-**9**.

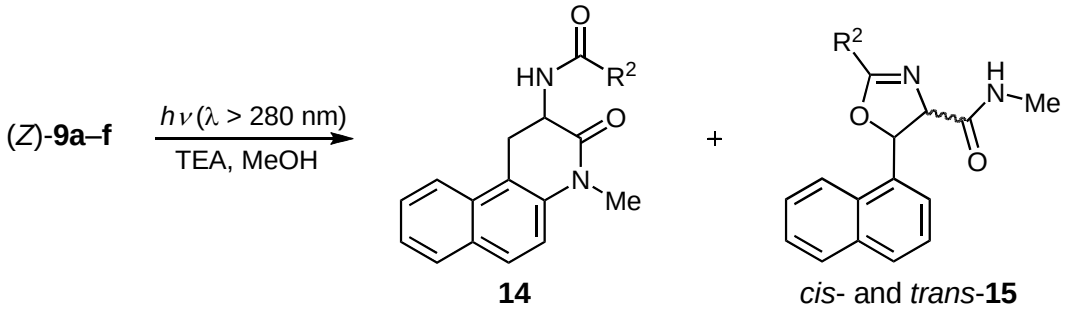

Scheme 9

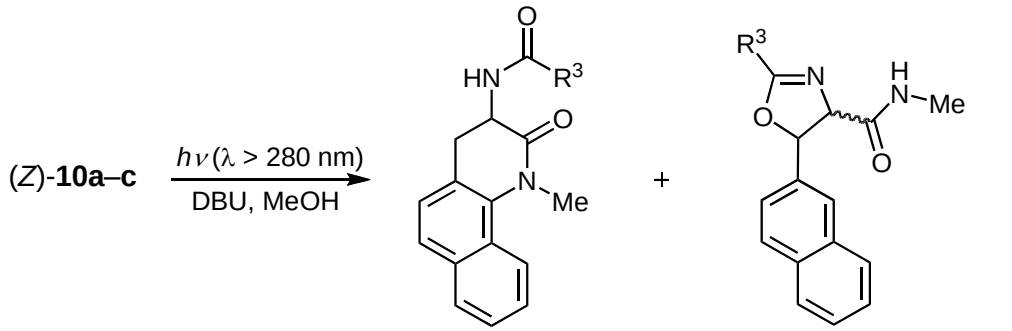

Scheme 10

We found that the free energy change for ET from TEA to (*E*)-**9e** [R^2 = 2,4-$(OMe)_2C_6H_3$] in the singlet excited state is –85 kJ mol^{-1}, and this excited-state (*E*)-isomer quantitatively yields dihydrobenzoquinolinone **14e**. These results enabled us to estimate relative rates for ET and related processes through the analysis of the TEA concentration dependence of quantum yield for the appearance of this cyclization product ($\Phi_{\mathbf{14e}}$, Scheme 11). The relative rates summarized in Table 5 demonstrate that the rate of ET (k_{et}) is faster than that of the deactivation and isomerization ($k_d + k_i$) of (*E*)-**9e** in the excited state by a factor of around 2, and that the rate of back ET (k_{-et}) is 14 times as fast as that of cyclization eventually affording **14e** ($k_{\mathbf{14e}}$). Therefore, analysis of these relative rates led to the conclusion that the relative rate $k_{-et}/k_{\mathbf{14e}}$ is a major factor that controls the overall efficiency of the PET-initiated cyclization reaction of (*E*)-**9e**.

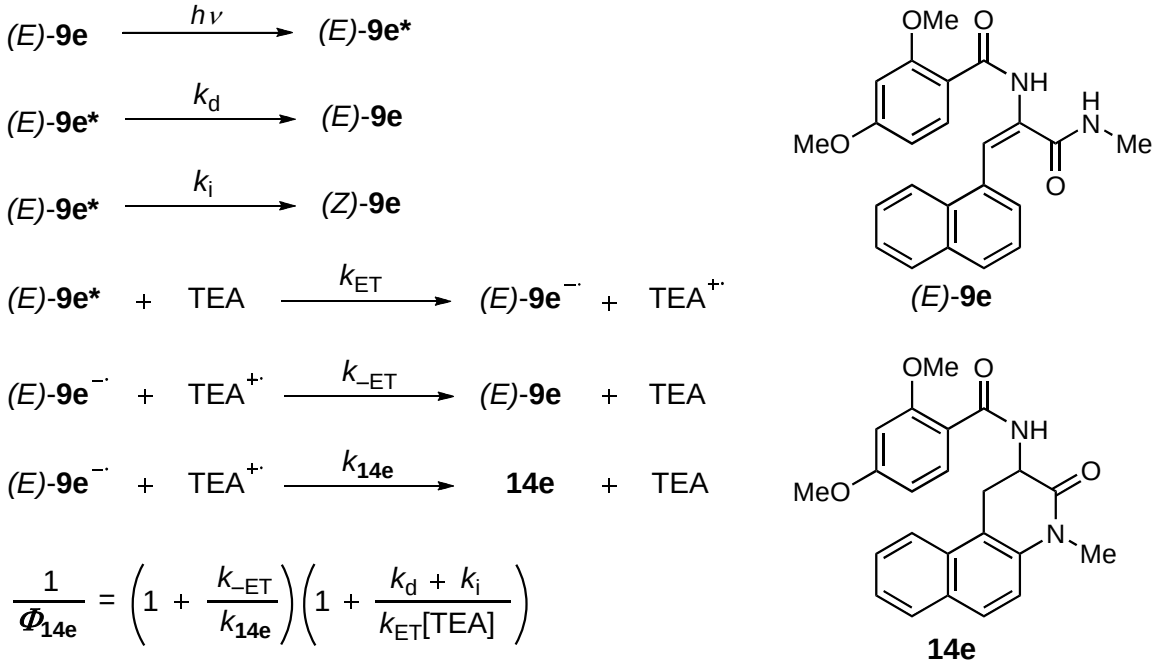

Scheme 11

Table 5. Relative rates for the quantum yield-determining processes ([TEA] = 0.10 mol dm^{-3})

$k_{-ET}/k_{\mathbf{14e}}$	$k_{ET}[TEA]/(k_d + k_i)$
14	1.9

To further expand the study of the PET-initiated cyclization reactions forming substituted dihydroquinolinones, (*Z*)-*N*-acyl-α-dehydro(methoxy-substituted phenyl)alanine *N′*-methylamides (*Z*)-**18a**–**g** were designed and synthesized in good yields (Figure 3). Irradiation of nitrogen-saturated methanol solutions containing these α-dehydroarylalaninamide derivatives and DBU gave nearly the same product distribution as that for (*Z*)-**9** (Scheme 12).

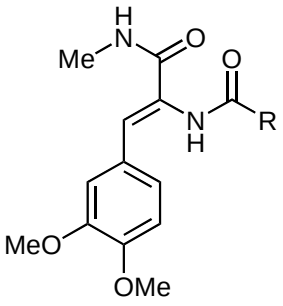

(*Z*)-**18a–g**

18a: R = Me
18b: R = *i*-Pr
18c: R = *t*-Bu
18d: R = $PhCH_2$
18e: R = 3,4-$Cl_2C_6H_3CH_2$
18f: R = 3,4-$(OMe)_2C_6H_3CH_2$
18g: R = 2,4-$(OMe)_2C_6H_3CH_2$

Figure 3. Structures of (*Z*)-**18a**–**g**

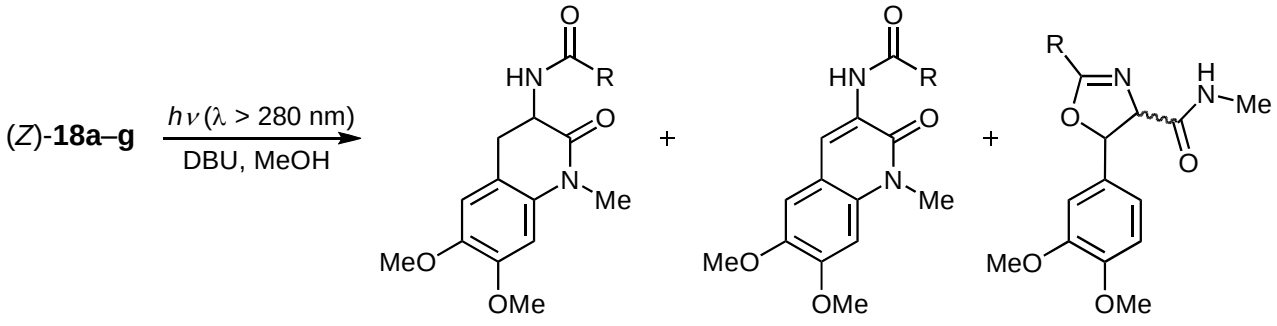

19 **20** *cis*- and *trans*-**21**

Scheme 12

When TEA was used instead of DBU as an electron donor, the conversion of **18a** decreased and the selectivity of **19a** also decreased with the increased selectivity of **20a**. The former finding confirms that α-dehydrophenylalaninamide derivative **18** is considerably less reactive than the corresponding

1-naphthylalaninamide derivative **9**. The latter finding is consistent with the involvement of two different modes of cyclization competitively forming **19** (selectivity: 82–94%) and **20**. The minor products **20** and **21** were readily removed by recrystallization from ethanol.

As described in sections 2-1 and 2-2, intramolecular and intermolecular PET-initiated cyclization reactions of various (*Z*)-*N*-acyl-α-dehydroarylalaninamides in methanol proceed cleanly and efficiently to produce the corresponding substituted 3,4-dihydrobenzoquinolinones in good to high yields, although these photochemical transformations experience significant steric hindrance. There are many synthetic routes to medium-sized lactams fused to an aromatic ring,[14] whereas convenient photochemical routes to these lactams are scarce.[15] Thus, our PET-initiated cyclization reactions present a novel method for constructing the 3,4-dihydroquinolinone ring.

2-3. 1,2,4-Triazole-substituted (*Z*)-α-dehydroarylalaninamides[16–18]

Hydrazides have frequently been utilized as convenient building blocks for creating various heterocyclic ring systems.[19] If we could introduce a hydrazide chromophore into an α-dehydroamino acid derivative, it would be possible to pave the way for a new mode of a PET-initiated cyclization reaction. When (*Z*)-2-methyl-4-(1-naphthylmethylene)-5-(4*H*)-oxazolone was allowed to react with an equimolar amount of acetohydrazide in acetonitrile, 1,2,4-triazole-substituted (*Z*)-2-propenoic acid derivative (*Z*)-**22a** was quantitatively obtained (Scheme 13). The X-ray crystal structure depicted in Scheme 13 provided definitive evidence for the structure of **22a** [hereafter, referred to as 1,2,4-triazole-substituted (*Z*)-α-dehydro(1-naphthyl)alanine].

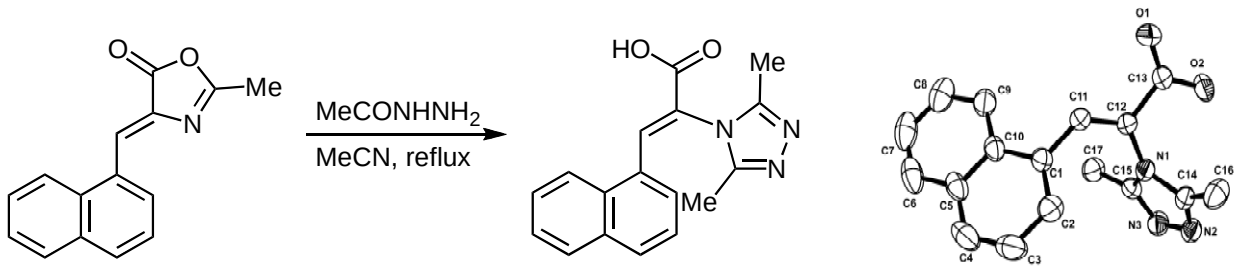

(*Z*)-**22a** Crystal structure of (*Z*)-**22a**

Scheme 13

The reactions of (*Z*)-2-methyl-4-arylmethylene-5-(4*H*)-oxazolones with several hydrazide nucleophiles led to the formation of the corresponding 1,2,4-triazole-substituted (*Z*)-α-dehydroarylalanines (*Z*)-**22a**–**m** in high yields (Table 6). Meanwhile, the observation that a small amount of the expected ring-opening product **23** was detected along with (*Z*)-**22** and (*E*)-**22** in the mixture of products obtained from the

Table 6. Isolated yields of (*Z*)-**22** and (*E*)-**22** obtained from the reactions of (*Z*)-2-methyl-4-arylmethylene-5(4*H*)-oxazolones with hydrazides in MeCN

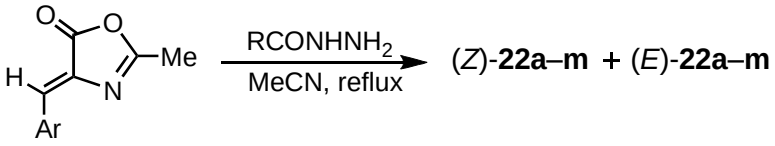

Product	Ar	R	Reaction time (h)	Isolated yield (%)	
				(Z)-**22**	*(E)*-**22**
22a	1-Np[a]	Me	0.5	90	Ñ [b]
22b	1-Np[a]	H	0.5	89	Ñ [b]
22c	1-Np[a]	Ph	1.0	80	Ñ [b]
22d	1-Np[a]	4-$OMeC_6H_4$	0.5	87	Ñ [b]
22e	1-Np[a]	4-CNC_6H_4	0.5	90	Ñ [b]
22f	1-Np[a]	4-$NO_2C_6H_4$	1.0	88	Ñ [b]
22g	1-Np[a]	$PhCH_2$	1.0	72	24
22h	Ph	Me	0.5	88	7
22i	Ph	H	0.5	97	Ñ [b]
22j	Ph	Ph	1.0	74	17
22k	Ph	4-$OMeC_6H_4$	0.5	57	20
22l	Ph	4-$NO_2C_6H_4$	1.0	92	Ñ [b]
22m	Ph	$PhCH_2$	1.0	75	15

[a] 1-Naphthyl. [b] Could not be detected.

reaction of the oxazolone with acetohydrazide suggests that this oxazolone has three sites for the nucleophilic addition of hydrazides, as shown in Scheme 14. The first site is the C=O double bond in the oxazolone ring, the second site is the C=N double bond in this ring, and the third site is the arylmethylene C=C double bond. A comparison of the heats of formation (ΔH_f) for the energy-minimized adducts **I** (ΔH_f for Ar = Ph, R = Me = –290.1 kJ mol^{-1}), **II** (–257.0 kJ mol^{-1}), and **III** (–272.8 kJ mol^{-1}) proves that the adduct **I** is the most stable intermediate; hence, its formation becomes a major process in the reaction. The ring-opening reaction with hydrazides is considered to be a thermodynamically controlled process.

Because little is known about the photochemical behavior of triazole derivatives,[20] we synthesized 1,2,4-triazole-substituted (*Z*)-α-dehydro(1-naphthyl)alaninamides (*Z*)-**24a**–**h** (Figure 4) and explored their PET-initiated cyclization reactions. When a nitrogen-saturated methanol solution containing (*Z*)-**24a** and TEA was irradiated at room temperature (internal irradiation), 1-methylbenzo[*f*]quinolinone (**25a**), 3,4-dihydrobenzo[*f*]quinolinone **26a**, and 3,5-dimethyl-1,2,4-triazole (**27a**) were isolated in 65%, 15%, and 40% yields, respectively (Scheme 15).

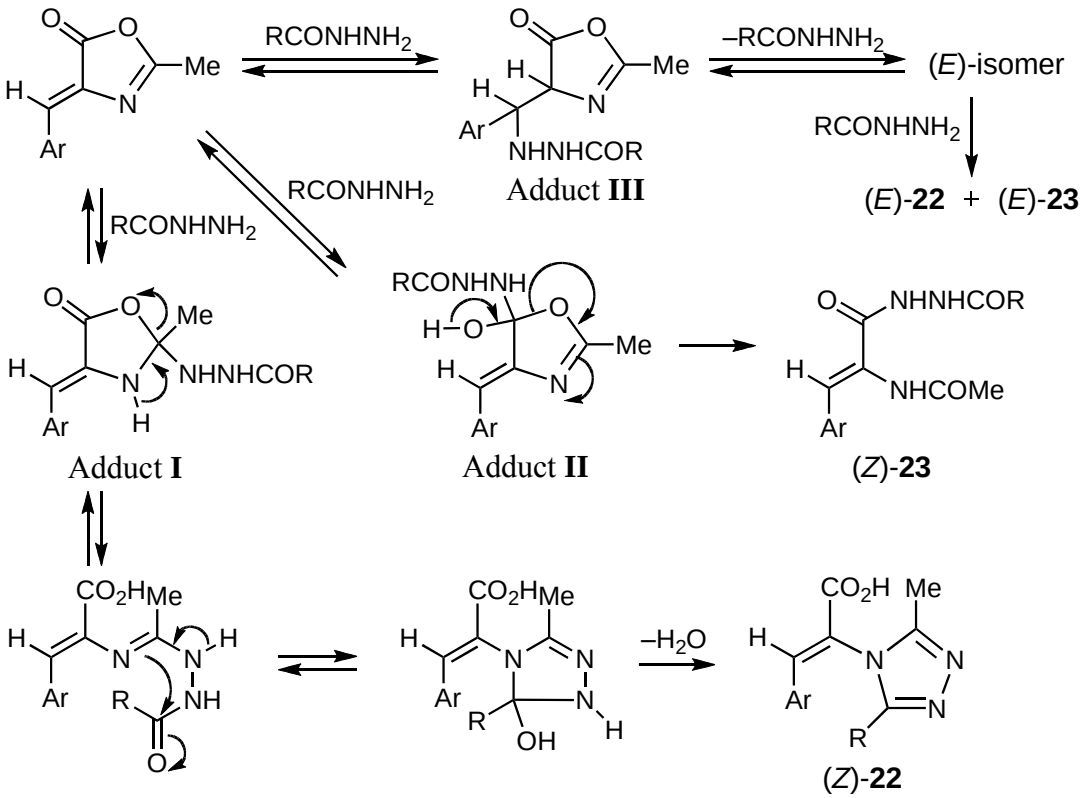

Scheme 14

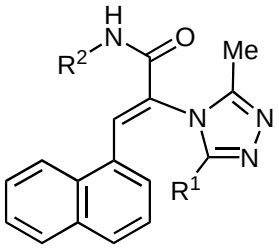

(*Z*)-**24a–h**

24a: $R^1 = R^2 = Me$
24b: $R^1 = H$, $R^2 = Me$
24c: $R^1 = PhCH_2$, $R^2 = Me$
24d: $R^1 = Ph$, $R^2 = Me$
24e: $R^1 = 4\text{-}OMeC_6H_4$, $R^2 = Me$
24f: $R^1 = 4\text{-}CNC_6H_4$, $R^2 = Me$
24g: $R^1 = Me$, $R^2 = H$
24h: $R^1 = Me$, $R^2 = PhCH_2$

Figure 4. Structures of (*Z*)-**24a–h**

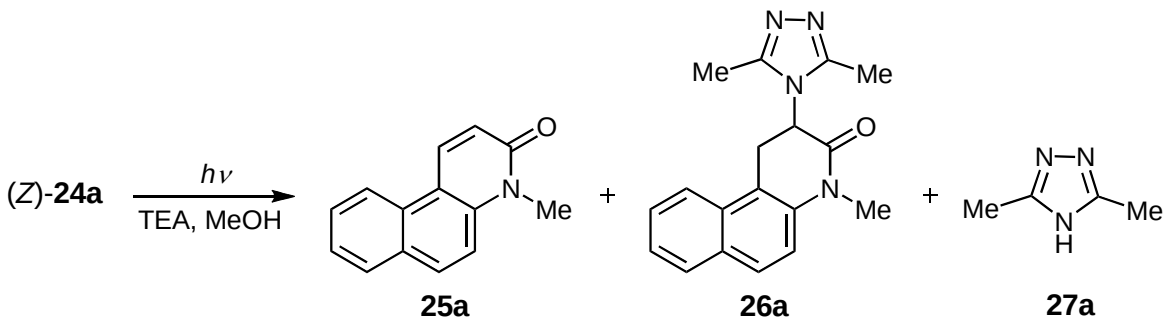

Scheme 15

Analysis of solvent and substituent effects on the composition ratio of **25** to **26**, summarized in Table 7, led us to propose that the relative composition of these cyclization products is controlled by an equilibrium between the initially formed 1-naphthylmethylene radical ion pair intermediates (*E*)-**IVA** and (*E*)-**IVB**, as depicted in Scheme 16.

Table 7. Solvent and substituent effects on the conversion of **24**, selectivity of **25** and **26**, and composition ratio of **25** to **26** at room temperature

(*Z*)-**24**	R^1	R^2	Solvent	Conversion (%)	Selectivity (%)		Composition ratio
					25	**26**	**25/26**
24a	Me	Me	MeOH	61	76	24	3.2
24a	Me	Me	EtOH	54	61	39	1.6
24a	Me	Me	*i*-PrOH	46	36	64	0.6
24a	Me	Me	MeCN	62	29	71	0.4
24a	Me	Me	CH_2Cl_2	65	18	82	0.2
24a	Me	Me	MeOH-H_2O (3:1 v/v)	44	80	20	4.0
24b	H	Me	MeOH	62	71	29	2.4
24c	$PhCH_2$	Me	MeOH	65	77	23	3.3
24d	Ph	Me	MeOH	61	86	14	6.1
24e	4-$OMeC_6H_4$	Me	MeOH	52	83	17	4.9
24f	4-CNC_6H_4	Me	MeOH	62	90	10	9.0
24g	Me	H	MeOH	48	63	37	1.7
24h	Me	$PhCH_2$	MeOH	52	77	23	3.3

On the other hand, the replacement of the 1-naphthyl group in (*Z*)-**24** by the methoxy-substituted phenyl ring [(*Z*)-**28a**–**c**, Figure 5] lowered the photoreactivity of the alaninamide derivative without exerting a great effect on the quinolinone selectivity.

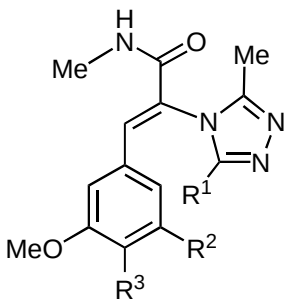

(*Z*)-**28a–c**

28a: R^1 = Me, R^2 = R^3 = H
28b: R^1 = Me, R^2 = H, R^3 = OMe
28c: R^1 = Ph, R^2 = OMe, R^3 = H

Figure 5. Structures of (*Z*)-**28a**–**c**

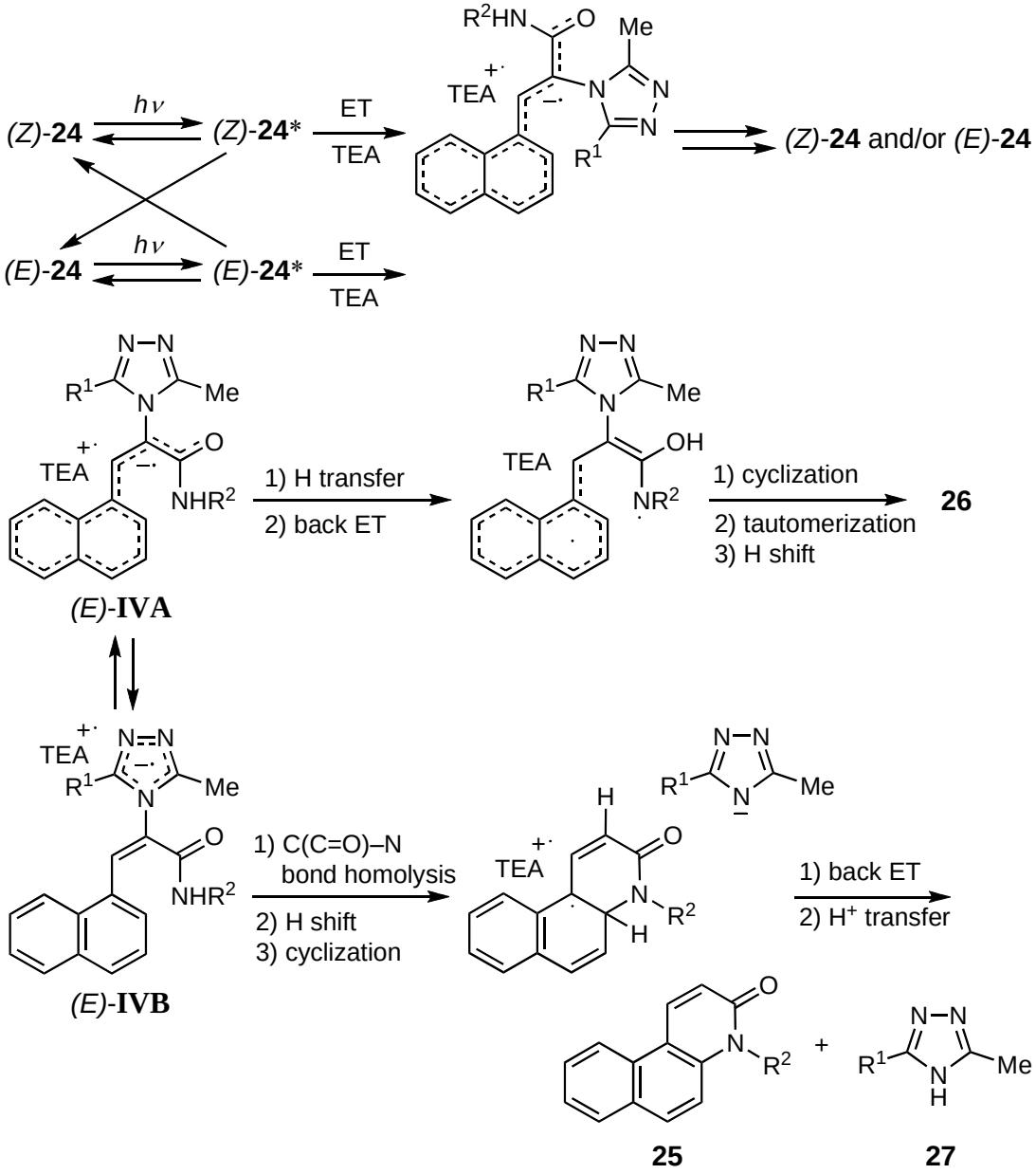

Scheme 16

Although there are several synthetic studies aimed at constructing the quinolinone ring,[21] only limited photochemical routes are available for this nitrogen-containing aromatic heterocycle.[22] Thus, the PET-initiated cyclization reactions of triazole-substituted (*Z*)-α-dehydroarylalaninamides provide a convenient method for synthesizing several quinolinone derivatives.

2-4. (*Z*)-*N*-Acyl-α-dehydroarylalanine alkyl esters[23–25]

We already showed that in the PET-initiated cyclization reactions of (*Z*)-*N*-acyl-α-dehydro(1-naphthyl)-alaninamides that produce the corresponding 3,4-dihydrobenzoquinolinone, benzoisoquinoline, and 4,5-dihydrooxazole derivatives, the replacement of the *N*-acetyl group by the *N*-benzoyl group greatly

lowered the benzoisoquinoline selectivity owing to the steric hindrance by the latter acyl group. Additionally, the *N′*-alkylamide nitrogen was shown to be involved in the dihydrobenzoquinolinone-forming cyclization process. Thus, it was predicted that (*Z*)-*N*-aroyl-α-dehydro(1-naphthyl)alanine alkyl esters (*Z*)-**29a**–**l** would undergo PET-initiated cyclization reactions to selectively afford the corresponding 4,5-dihydrooxazoles (Figure 6).

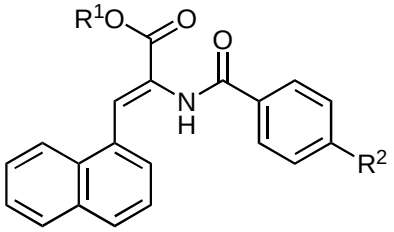

(*Z*)-**29a–e**

29a: R^1 = Me, R^2 = H
29b: R^1 = *i*-Pr, R^2 = H
29c: R^1 = *t*-Bu, R^2 = H
29d: R^1 = Me, R^2 = OMe
29e: R^1 = Me, R^2 = CN

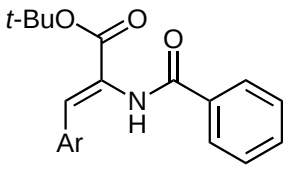

(*Z*)-**29f–l**

29f: Ar = 4-$OMeC_6H_4$
29g: Ar = 4-MeC_6H_4
29h: Ar = Ph
29i: Ar = 4-ClC_6H_4
29j: Ar = 4-CNC_6H_4
29k: Ar = 2-MeC_6H_4
29l: Ar = 2,6-$Me_2C_6H_3$

Figure 6. Structures of (*Z*)-**29a**–**l**

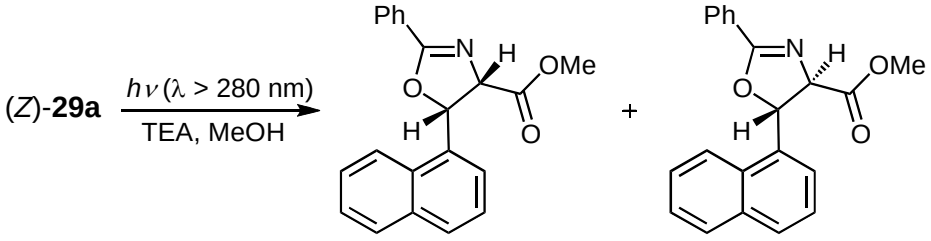

cis-**30a** *trans*-**30a**

Scheme 17

After a nitrogen-saturated methanol solution containing (*Z*)-**29a** and TEA was irradiated for a set period of time at room temperature, standard workup of the reaction mixture allowed us to almost quantitatively isolate *cis*- and *trans*-4-methoxycarbonyl-5-(1-naphthyl)-2-phenyl-4,5-dihydrooxazoles (*cis*-**30a** and *trans*-**30a**, Scheme 17). This result is consistent with our prediction and the unambiguous structure of these two photoproducts was provided by X-ray single-crystal structural analysis, as depicted in Figure 7. We unexpectedly found that the compositon ratio of *cis*-**30a** to *trans*-**30a** decreases with irradiation time, suggesting the occurrence of the TEA-catalyzed isomerization of the *cis*-isomer to the thermodynamically more stable *trans*-isomer (see Scheme 18). This isomerization was substantiated by a control study

showing that *cis*-**30a** slowly isomerized in the presence of TEA to furnish a 9:1 equilibrium mixture of the *trans*- and *cis*-isomers, respectively. The observed isomerization also confirms the involvement of a carbanion intermediate in this process.

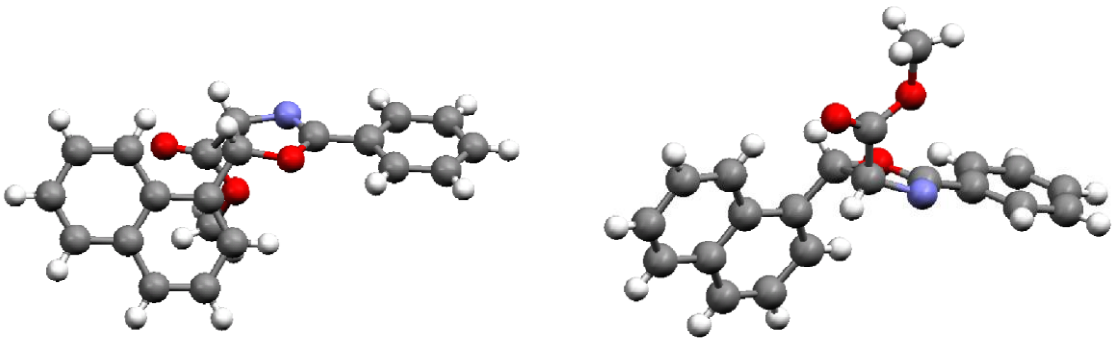

cis-**30a** *trans*-**30a**

Figure 7. Crystal structures of *cis*-**30a** and *trans*-**30a**

The use of the reduction potential of **29a** (E_{red} = –2.26 eV vs. Ag/AgCl in MeCN), the oxidation potential of TEA (E_{ox} = 0.76 V), and the first singlet excitation energy of **29a** (E_S = 368 kJ mol^{-1}) enabled the estimation of the free energy change (ΔG_{et}) for ET from TEA to this singlet excited-state α-dehydronaphthylalanine methyl ester as –77 kJ mol^{-1}, on the basis of the simplified Weller equation: $\Delta G_{et} = 96.5(E_{ox} - E_{red}) - E_S$. The additional finding that the fluorescence intensity of (*Z*)-**29a**–**e** is considerably reduced with increasing electron-withdrawing ability of the substituent R^2 attached to the *N*-benzoyl benzene ring confirms the formation of the acyl radical anion intermediate in a stepwise manner, as shown in Scheme 18.

As already discussed, 4,5-dihydrooxazole derivatives **30** are likely produced through the (*E*)-**29**-derived radical ion pair intermediate (*E*)-**VB**. In this scheme, significant steric hindrance by the bulky naphthyl group bonded at the 5-position of the oxazole ring causes a hydrogen shift in the biradical intermediate **VI** to proceed from the opposite side of this group, preferentially forming *cis*-**30**. Thus, the hydrogen shift can be regarded as a kinetically controlled process. Additionally, because the introduction of the bulky *tert*-butyl group into the alkoxy carbonyl moiety produces the corresponding *cis*-isomers with high selectivity without undergoing any TEA-catalyzed *cis* → *trans* isomerization (Table 8), the use of *N*-acyl-α-dehydroarylalanine *tert*-butyl esters (*Z*)-**29f**–**l** enables a discussion about the substituent effects on the *cis*-**30** selectivity and photoreactivity of the starting **29**.

As shown in Table 9, the *cis*-isomer selectivity has a clear tendency to increase with an increase in the steric bulk of the aryl substituents. Moreover, the photoreactivity (conversion) of **29** decreases in the

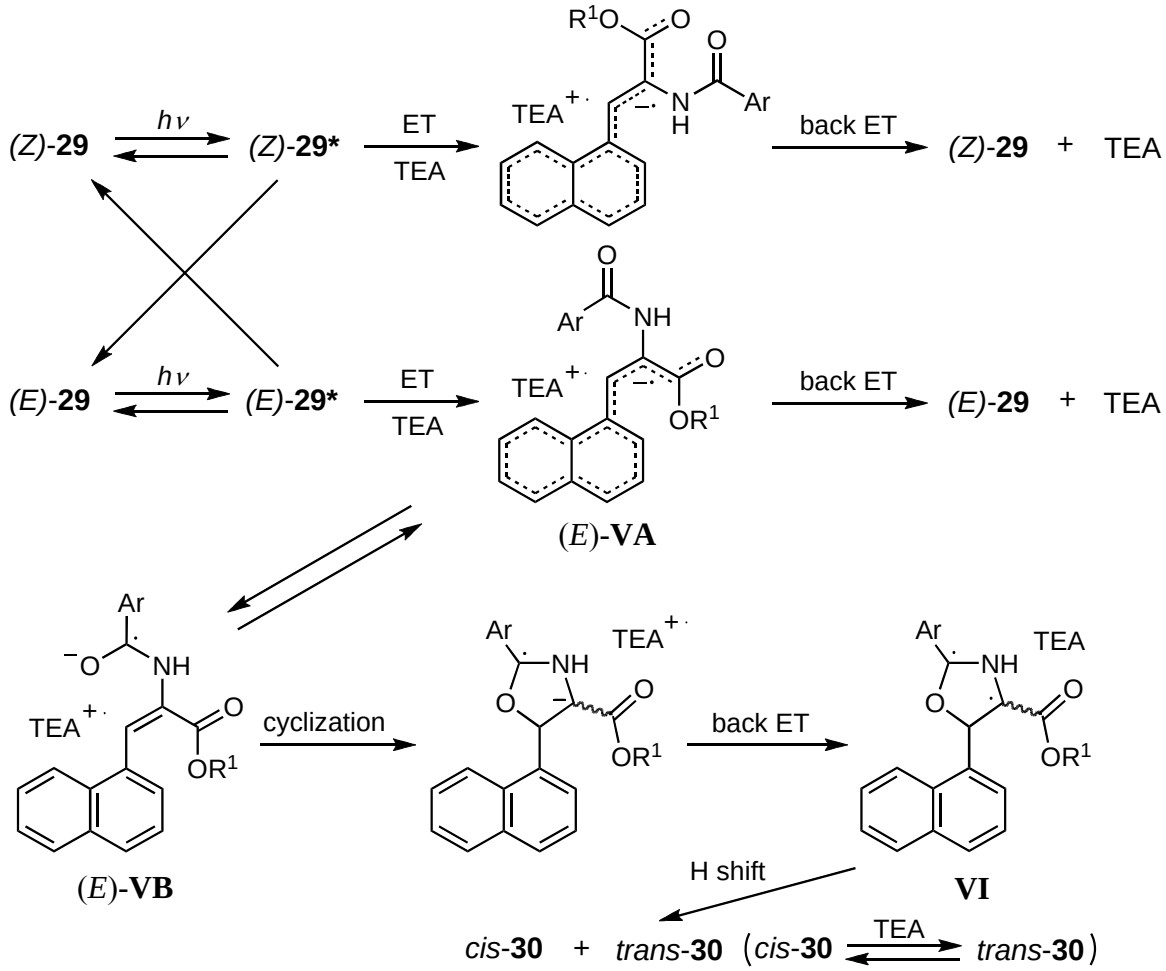

Scheme 18

Table 8. Substituent effects on the conversion of **29a**–**e** and selectivity of *cis*-**30a**–**e** in MeOH at room temperature

(*Z*)-**29**	Irradiation time (h)	Conversion (%)	Composition (%)		Selectivity (%)
			cis-**30**	*trans*-**30**	
29a	0.5	16.5	11.5	5.0	70
	5	100.0	36.9	63.1	37
29b	0.5	18.9	16.5	2.4	87
	5	100.0	80.9	19.1	81
29c	0.5	20.0	18.4	1.6	92
	5	100.0	91.5	8.5	92
29d	0.5	12.6	9.8	2.8	78
	5	92.7	60.6	32.1	65
29e	0.5	9.0	4.6	4.4	51
	5	75.4	13.5	61.9	18

Table 9. Substituent effects on the conversion of **29f**Ğ and selectivity of *cis*-**30f**Ğ in MeOH at room temperature

(*Z*)-**29**	Irradiation time (h)	Conversion[a] (%)	Composition (%)		Selectivity (%)
			cis-**30**	*trans*-**30**	
29f	0.5	5.1	4.1	1.0	80
	3	30.9	24.5	6.4	79
29g	0.5	6.3	5.0	1.3	79
	3	37.1	29.0	8.1	78
29h	0.5	6.6	5.1	1.5	77
	3	40.8	31.6	9.2	77
29i	0.5	9.5	7.1	2.4	75
	3	57.6	42.5	15.1	74
29j	0.5	7.4	5.0	2.4	68
	3	42.2	23.0	19.2	55
29k	0.5	4.9	4.7	0.2	96
	3	29.8	28.5	1.3	96
29l	0.5	2.1	2.1	0	100
	3	14.0	14.0	0	100

following order: **29c** (Ar = 1-naphthyl) > **29h** (Ar = phenyl) > **29l** (Ar = 2,6-$Me_2C_6H_3$), and this reactivity tends to be enhanced with increased electron-withdrawing ability of the aromatic acyl group. These results suggest that the reactivity is mainly determined by intermolecular electron transfer efficiency from TEA to **29** in the excited state, intramolecular ET efficiency from the 1-naphthylmethylene radical anion to the aromatic acyl group in (*E*)-**VA**, and steric hindrance to the cyclization process of the radical ion pair intermediate (*E*)-**VB** (Scheme 18).

There are several synthetic routes to 4,5-dihydrooxazole derivatives, but a convenient photochemical route to these derivatives has not yet been developed.[26] The PET reactions described above efficiently proceed to quantitatively afford *cis*- and *trans*-4,5-dihydrooxazoles, and the composition ratio of these two cyclization products can be controlled by utilizing the steric and electronic effects of the alkyl and aryl substituents introduced into (*Z*)-**29**. Therefore, the PET-initiated cyclization reactions of (*Z*)-*N*-acyl-α-dehydronaphthylalanine alkyl esters constitute a novel photochemical method for constructing a pharmaceutically useful 4,5-dihydrooxazole ring.

On the basis of the photocyclization mode, according to which α-dehydro(1-naphthyl)alanine alkyl esters (*Z*)-**29** are converted into substituted 4,5-dihydrooxazoles **30**, we predict that the replacement of the

N′-amide hydrogen in (*Z*)-*N*-benzoyl-α-dehydro(1-naphthyl)alanine *N′*-alkylamides by an alkyl group would funnel the corresponding *N′*,*N′*-dialkylamide derivatives (*Z*)-**31a**,**b** toward the 4,5-dihydrooxazole heterocycles by eliminating the pathway to the 3,4-dihydroquinolinones (Figure 8).

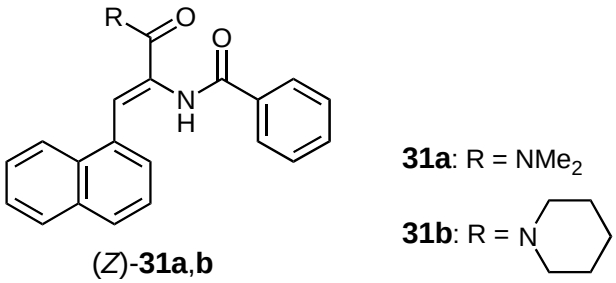

(*Z*)-**31a**,**b**

Figure 8. Structures of (*Z*)-**31a**,**b**

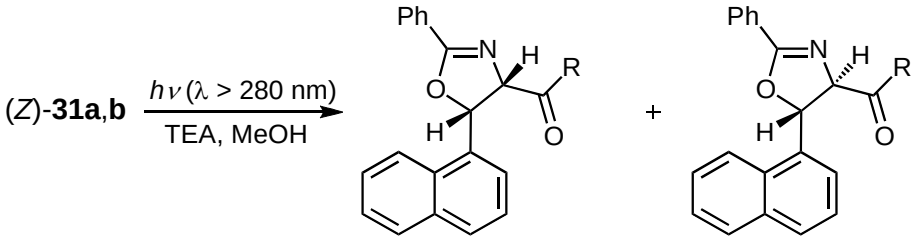

cis-**32** *trans*-**32**

Scheme 19

The PET reactions of (*Z*)-**31** in nitrogen-saturated methanol containing TEA less efficiently proceeded than those of the corresponding 1-naphthylalanine *tert*-butyl esters to produce *cis*-4,5-dihydrooxazole derivatives *cis*-**32** in preference to *trans*-**32** as predicted (Scheme 19). Additionally, the use of 1,2-dichloroethane as a solvent greatly enhanced the *cis*-isomer selectivity and photoreactivity of the starting α-dehydronaphthylalaninamides under the same irradiation conditions.

3. ACHIRAL AMINE- AND CHIRAL AMINE-CATALYZED ASYMMETRIC PHOTOCYCLIZATION REACTIONS

3-1. Chiral auxiliary-substituted (*Z*)-*N*-acyl-α-dehydroarylalaninamides[27–29]

As described in the preceding chapter, the PET-initiated cyclization reactions of (*Z*)-*N*-acyl-α-dehydroarylalaninamides cleanly proceeded to construct the dihydroquinolinone ring in high selectivity. Because this heterocyclic ring possesses an asymmetric carbon at the 3-position, it is possible to develop our PET-initiated reactions into diastereoselective cyclizations by introducing various chiral auxiliary

groups into the starting α-dehydroarylalaninamides. To find a new type of asymmetric photocyclization and shed more light on the dihydroquinolinone ring formation mechanism, we synthesized (*Z*)-*N*-acyl-α-dehydro(1-naphthyl)alaninamides bearing the (*S*)-alanine methyl ester auxiliary group, (*Z*)-**33a**,**b** (Figure 9) and calculated the diastereomeric excess (de) of each of the corresponding 3,4-dihydrobenzo[*f*]quinolinone derivatives formed under several cyclization conditions.

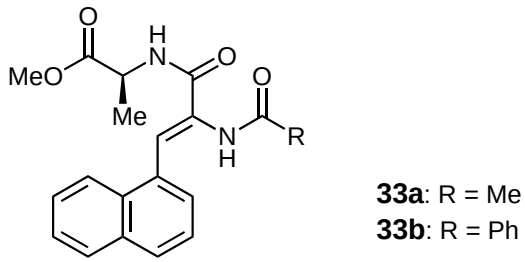

(*Z*)-**33a**,**b**

Figure 9. Structures of (*Z*)-**33a**,**b**

Irradiation of a nitrogen-saturated methanol solution containing (*Z*)-**33** and TEA led to the formation of the 3,4-dihydrobenzoquinolinone diastereomers (*S*,*S*)-**34** and (*R*,*S*)-**34**, along with benzoisoquinoline derivative **35** (Scheme 20). On the basis of the absolute configuration of one of these two diastereomers (*R*,*S*)-**34b**, shown in Figure 10, and the chemical shifts of their methine proton NMR signals, we could determine the compositions and de of (*S*,*S*)-**34** and (*R*,*S*)-**34**, which were collected in Table 10.

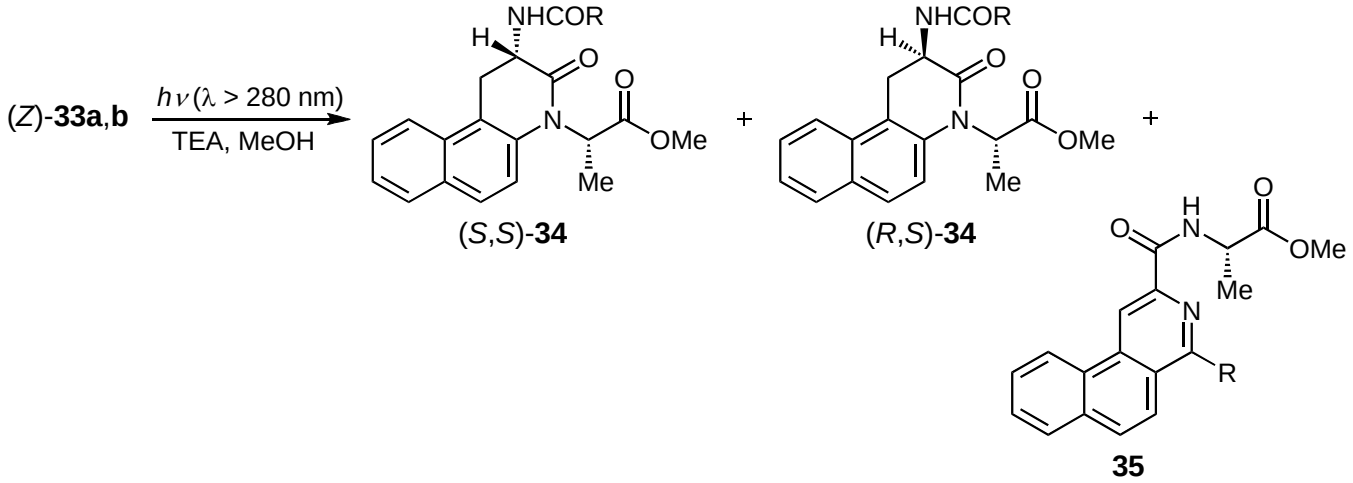

Scheme 20

Inspection of the data in this Table reveals that the increased steric bulk of the tertiary amine significantly lowers the de for the (*S*,*S*)-diastereomer formed in excess; the decreased hydrogen-bonding solvation ability of methanol has a clear tendency to substantially enhance the de for this diastereomer. As

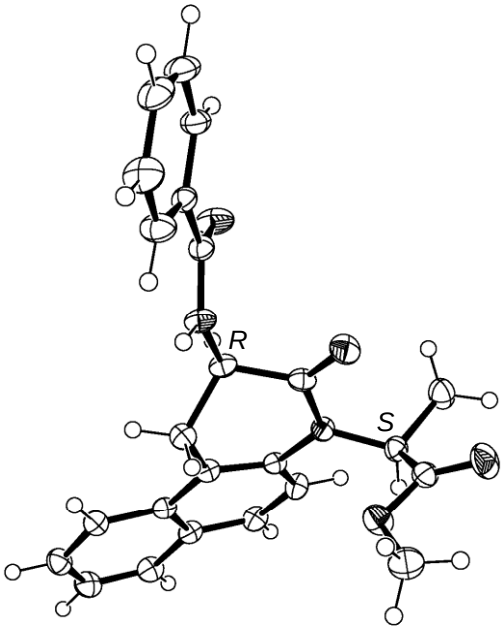

Figure 10. Crystal structure of (*R*,*S*)-**34b**

Table 10. Effects of chiral auxiliary, tertiary amine, and solvent on the conversion of **33**, selectivity of **34**, and diasteremeric excess for (*S*,*S*)-**34** at room temperature

(*Z*)-**33**	Tertiary amine	Solvent	Conversion (%)	Selectivity (%)	Composition (%)		de (%)
					(*S*,*S*)-**34**	(*R*,*S*)-**34**	
33a	TEA	MeOH	79	49	21.1	17.6	9
33b	TEA	MeOH	46	45	11.7	9.0	13
33a	TMA[a]	MeOH	72	48	20.4	14.2	18
33a	MP[b]	MeOH	74	52	25.2	13.3	31
33a	PEP[c]	MeOH	65	55	17.9	17.9	0
33b	MP	MeOH	70	20	9.5	4.5	36
33a	TEA	MeOH-MeCN (1:1 v/v)	82	30	15.5	9.1	26
33a	TEA	MeOH-MeCN (1:9 v/v)	63	9	4.4	1.3	54
33a	MP	MeOH-MeCN (1:9 v/v)	67	13	6.3	2.4	45

[a]Trimethylamine.
[b]1-Methylpiperidine.
[c]*N*-Isopropyl-*N*-ethylisopropylamine.

discussed in the preceding chapter, the asymmetric carbon at the 3-position of the dihydroquinolinone ring is likely generated through the tautomerization of the corresponding enol intermediate (Scheme 8). In addition, energy-minimized conformations of this intermediate containing the *N*-benzoyl group are very similar to the X-ray crystal structure of (*R*,*S*)-**34b** (Figure 11), confirming that the methoxycarbonyl group in the (*S*)-alanyl chiral auxiliary is preferentially directed to the *re* face; hence, there is a difference in the extent of hydrogen bonding and electrostatic interactions of the tertiary amine with the enol intermediate between the two diastereofaces. It is likely that more favorable hydrogen bonding and electrostatic interactions in the *re*-face side of this intermediate force the enol hydroxy proton to add to the olefinic carbon preferentially from the *re* face, affording the (*S*,*S*)-diastereomer in excess, as depicted in Scheme 21.

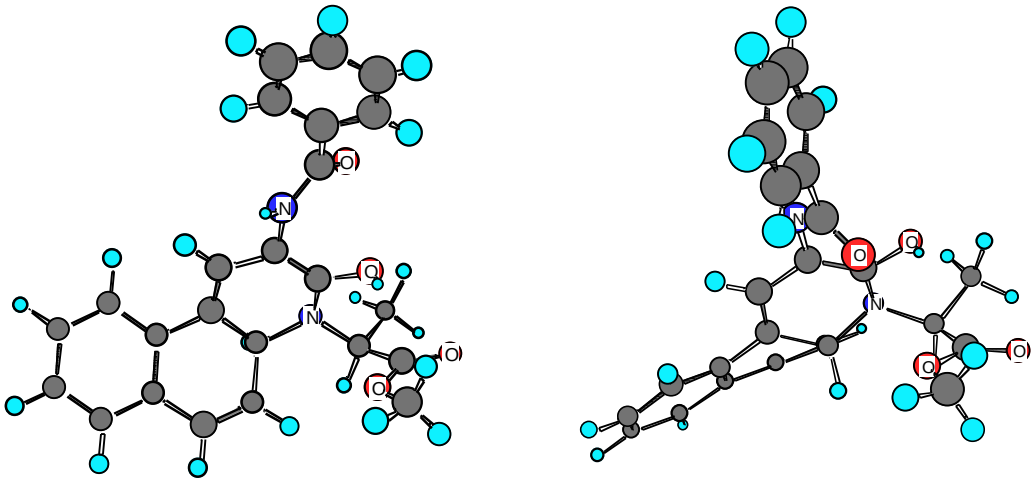

Figure 11. Energy-minimized conformations of the **33b**-derived enol intermediates

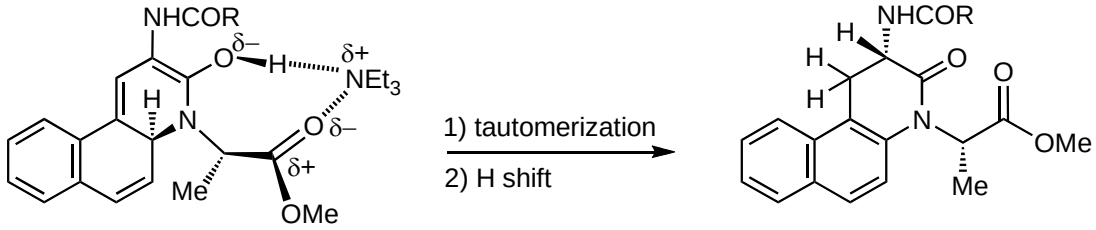

enol intermediate (R = Me, Ph) (*S*,*S*)-**34**

Scheme 21

Because the conformation of the chiral auxiliary in the enol intermediate clearly plays an essential role in controlling the configuration and de of the diastereomer formed in excess, the use of the (*S*)-alaninamide-type chiral auxiliaries shown in Figure 12 was expected to exert a great effect on the stereochemistry of enol → keto tautomerization. Irradiation of a nitrogen-saturated methanol solution containing (*Z*)-**36a** and TEA at room temperature led to the formation of 3,4-dihydrobenzoquinolinones

(*S*,*S*)-**37a** and (*R*,*S*)-**37a** with higher selectivity (71%) than that (49%) for the **33a**-derived dihydroquinolinone, along with benzoisoquinoline **38a** and 4,5-dihydrooxazole **39a** (Scheme 22).

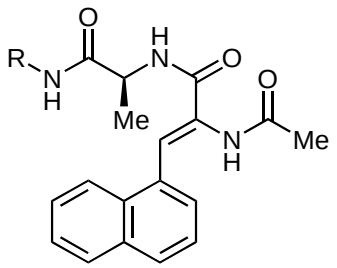

(*Z*)-**36a–f**

36a: R = Me
36b: R = H
36c: R = *t*-Bu
36d: R = Ph
36e: R = 4-OMeC$_6$H$_4$
36f: R = 4-CNC$_6$H$_4$

Figure 12. Structures of (*Z*)-**36a–f**

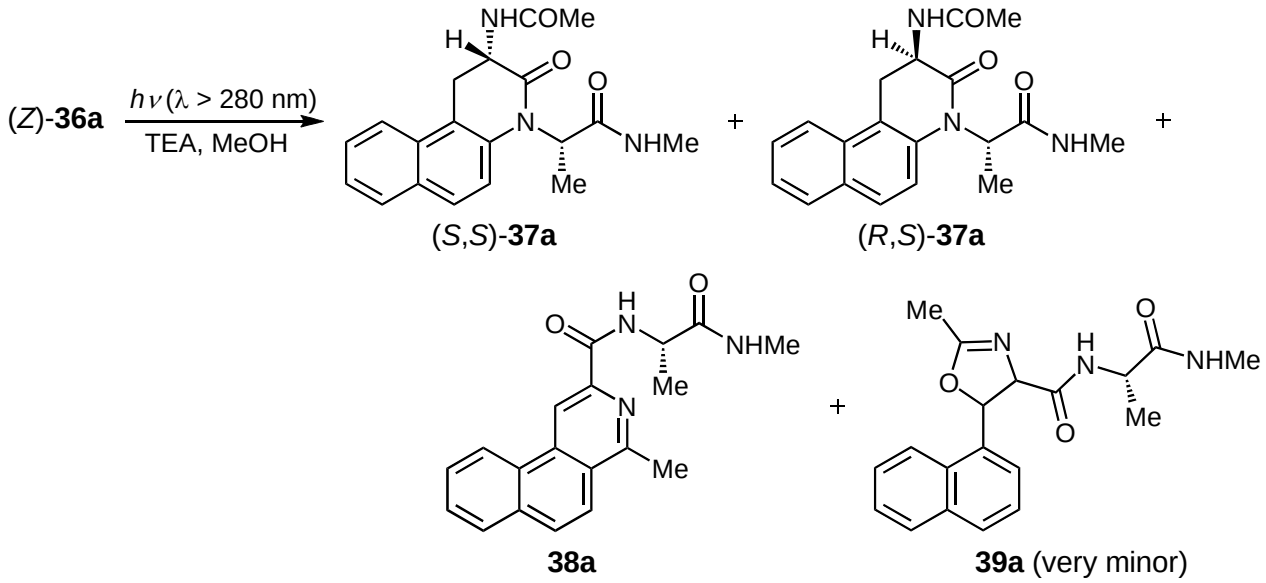

Scheme 22

On the basis of the sign of the 255-nm circular dichroism (CD) bands for (*S*,*S*)-**37** and (*R*,*S*)-**37** and the ^{1}H NMR spectral data of these diastereomers, the de value of the major diastereomer was determined. The effects of the substituent, solvent, tertiary amine, and reaction temperature on the selectivity and de of **37** were summarized in Table 11. In contrast to the asymmetric photocyclization behavior of (*S*)-alanine methyl ester auxiliary-substituted derivatives (*Z*)-**33**, the temperature exerted a great effect on the de, whereas this de was only slightly affected by the steric bulk of the amine and the solvent. These findings suggest that the aforementioned hydrogen bonding and electrostatic interactions between the amine and the enol intermediate make a negligible contribution to asymmetric induction observed in the cyclization process of (*S*)-alaninamide auxiliary-substituted derivatives (*Z*)-**36**.

Table 11. Effects of Substituent, solvent, tertiary amine, and temperature on the conversion of **36**, selectivity of **37**, and diastereomeric excess (de) for (*S*,*S*)-**37** formed in excess

(*Z*)-**36**	Solvent	Amine	Temperature	Conversion (%)	Selectivity (%)	de (%)
36a	MeOH	TEA	50 ¡C	31	41	16
36a	MeOH	TEA	rt	40	71	34
36a	MeOH	TEA	Ğ78 ¡C	65	95	72
36a	MeOH	MP	rt	36	71	40
36a	MeOH	PEP	rt	39	73	34
36a	MeOH-MeCN (1:9 v/v)	TEA	rt	13	18	32
36b	MeOH	TEA	rt	43	68	38
36b	MeOH	TEA	Ğ78 ¡C	55	87	68
36c	MeOH	TEA	rt	29	41	33
36c	MeOH	TEA	Ğ78 ¡C	37	95	66
36d	MeOH	TEA	rt	32	54	52
36d	MeOH	TEA	Ğ78 ¡C	39	94	80
36e	MeOH	TEA	rt	31	53	57
36e	MeOH	TEA	Ğ78 ¡C	38	95	76
36f	MeOH	TEA	rt	30	67	70
36f	MeOH	TEA	Ğ78 ¡C	42	97	92

A marked temperature dependence of de and a large difference in thermodynamic stability between the cyclized enol intermediates **VIIIA** (ΔH_f for R = Me = –300.8 kJ mol^{-1}) and **VIIIB** (–294.4 kJ mol^{-1}), shown in Scheme 23, led us to suggest two conclusions: a pre-equilibrium exists between the enol biradical intermediates **VIIA** and **VIIB**, and steric repulsion between the methyl hydrogen in the chiral auxiliary and/or the naphthalene ring hydrogen at its 2-position and the enol hydroxy hydrogen is a predominant factor determining both the major diastereomer formed and the position of this pre-equilibrium. Higher thermodynamic stability of **VIIIA** (that shifts the pre-quilibrium to the **VIIA** side) and enol $\rightarrow$ keto tautomerization (that preferentially proceeds from the *re* face in **VIIIA**) are consistent with the preferential formation of the (*S*,*S*)-diastereomer (Table 11). Additionally, the alkyl and aryl substituents incorporated into the chiral auxiliaries are considered to affect the relative stability of **VIIIA** and **VIIIB**. The use of an (*S*)-alanine *N*′-(4-cyanophenyl)amide auxiliary enhanced de for (*S*,*S*)-**37** up to 92%.

3-2. (*Z*)-*N*-Acetyl-α-dehydro(1-naphthyl)alaninamides[30]

In the preceding section, we demonstrated that in addition to the relative stability of the diastereomeric

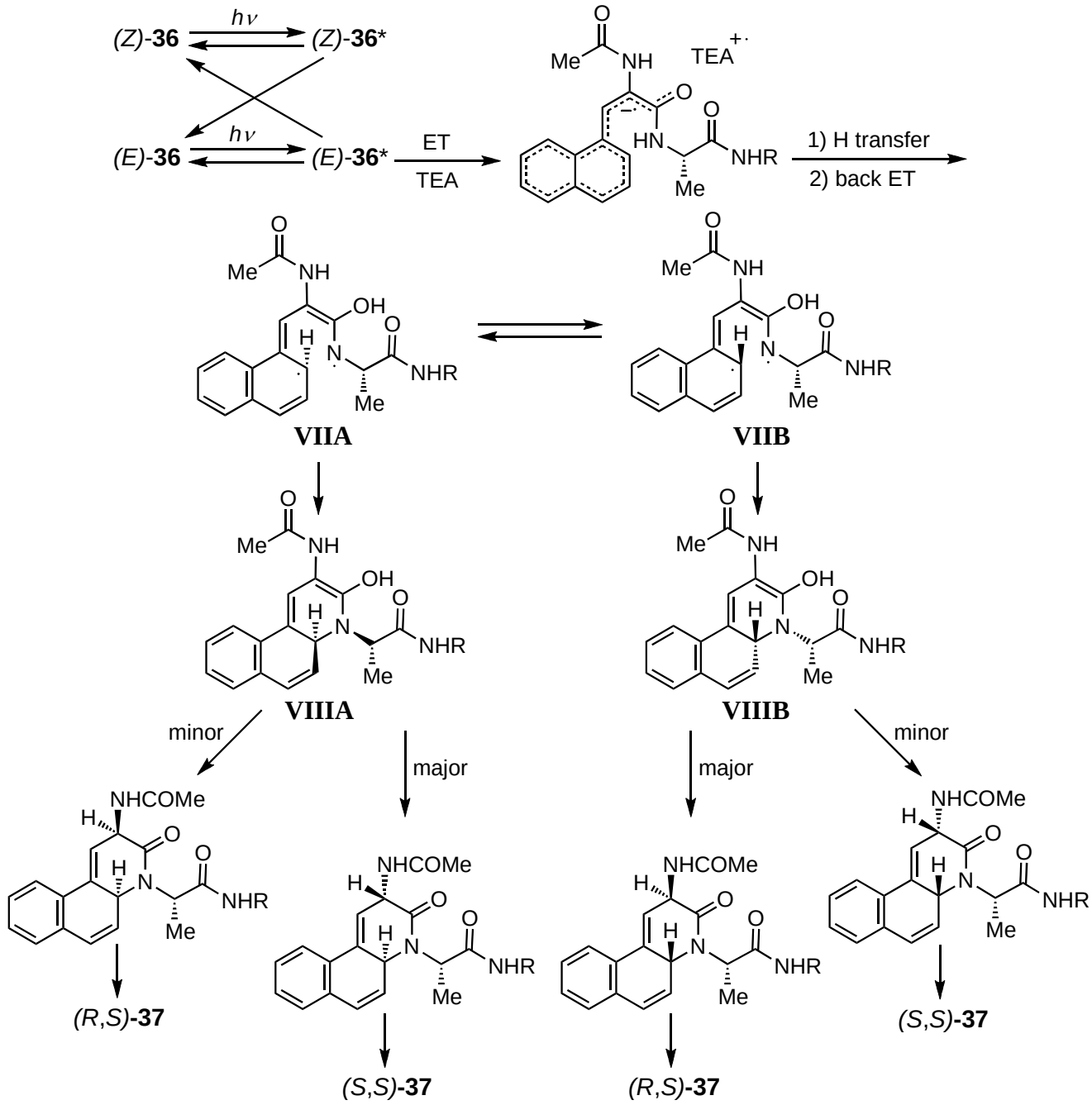

Scheme 23

enol intermediate, hydrogen bonding and electrostatic interactions between the tertiary amine and this intermediate are factors controlling the magnitude of de for the observed diastereoselective photocyclization. The latter finding makes it possible to design an enantioselective photocyclization of *N*-acyl-α-dehydro(1-naphthyl)alaninamides in the presence of a chiral amine. To develop a new type of asymmetric photocyclization, nitrogen-saturated 2-propanol or dichloromethane solutions containing α-dehydroamino acid amides (*Z*)-**40a**–**d** and (*S*)-1-methyl-2-pyrrolidinemethanol (S-MPM) or (*S*)-nicotine (S-NT) were irradiated at room temperature and –78 °C (Figure 13).

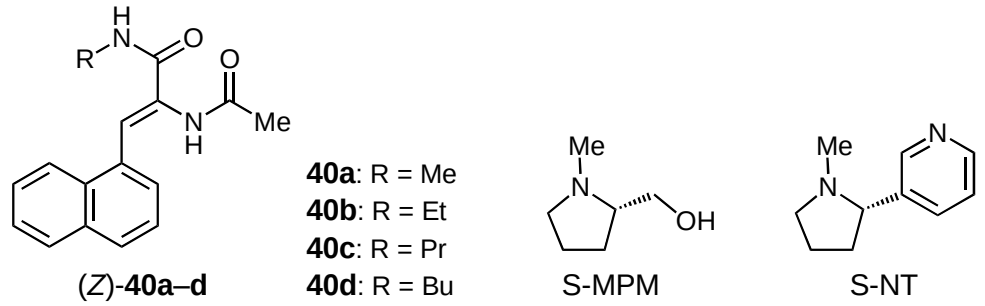

Figure 13. Structures of (*Z*)-**40a**–**d**, S-MPM, and S-NT

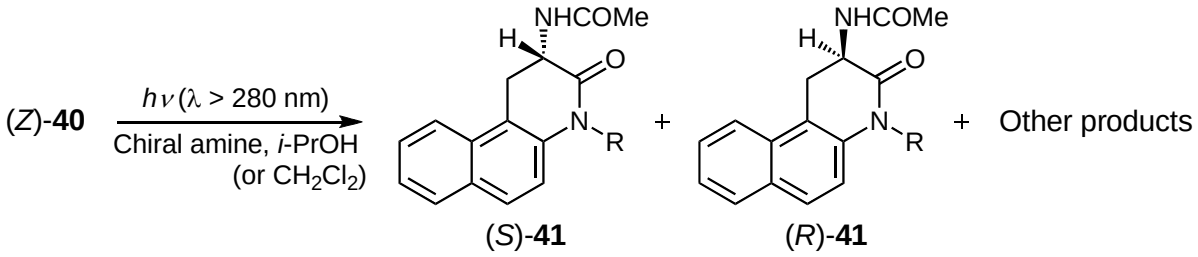

Scheme 24

Table 12. Effects of Chiral amine, solvent, temperature, and substituent effects on the conversion of **40**, selectivity of **41**, and ee for (*S*)-**41** or (*R*)-**41**

(*Z*)-**40**	Amine	Solvent	Temperature	Conversion (%)	Selectivity (%)	ee (%)	Major enantiomer
40a	MPM	*i*-PrOH	rt	94	57	7	*R*
40a	MPM	CH_2Cl_2	rt	96	31	30	*R*
40a	NT	*i*-PrOH	rt	95	41	23	*S*
40a	NT	CH_2Cl_2	rt	100	9	21	*S*
40a	MPM	*i*-PrOH	Ğ78 ¡C	57	95	9	*R*
40a	MPM	CH_2Cl_2	Ğ78 ¡C	67	82	34	*R*
40a	NT	*i*-PrOH	Ğ78 ¡C	52	90	59	*S*
40a	NT	CH_2Cl_2	Ğ78 ¡C	34	24	34	*S*
40b	NT	*i*-PrOH	Ğ78 ¡C	50	82	55	*S*
40c	NT	*i*-PrOH	Ğ78 ¡C	42	80	54	*S*
40d	NT	*i*-PrOH	Ğ78 ¡C	46	63	46	*S*

The absolute configuration of 3,4-dihydrobenzo[*f*]quinolinone products (*S*)-**41** and (*R*)-**41** obtained by irradiation at room temperature or –78 °C was determined by separating the **40**-derived enantiomeric

product mixture into the (*S*)- and (*R*)-enantiomers using a chiral HPLC column, followed by measuring their CD spectra (Scheme 24). The effects of chiral amine, solvent, temperature, and substituent on the enantiomeric excess (ee), summarized in Table 12, reveal that the use of S-MPM induces an asymmetric photocyclization reaction of (*Z*)-**40a** to produce (*R*)-**41a** in 7% ee (*i*-PrOH) and 30% ee (CH_2Cl_2), whereas the change of chiral amine to S-NT reverses the configuration of the major enantiomer with an accompanying remarkable enhancement in ee in 2-propanol at room temperature (7% → 23%).

Furthermore, the lowering of temperature enhanced selectivity and ee for (*S*)-**41a** in all solvents, although ee for the (*R*)-enantiomer formed in excess was only slightly increased by this temperature depression, substantiating the participation of a different mode of hydrogen-bonding interaction by S-NT and S-MPM. The data in Table 12 also show that an increase in the steric bulk of the substituent R has a clear tendency to diminish ee for (*S*)-**41**; hence, the amide N–H hydrogen is involved in the hydrogen bonding between S-NT and the enol intermediates **IX** and **X** (Scheme 25).

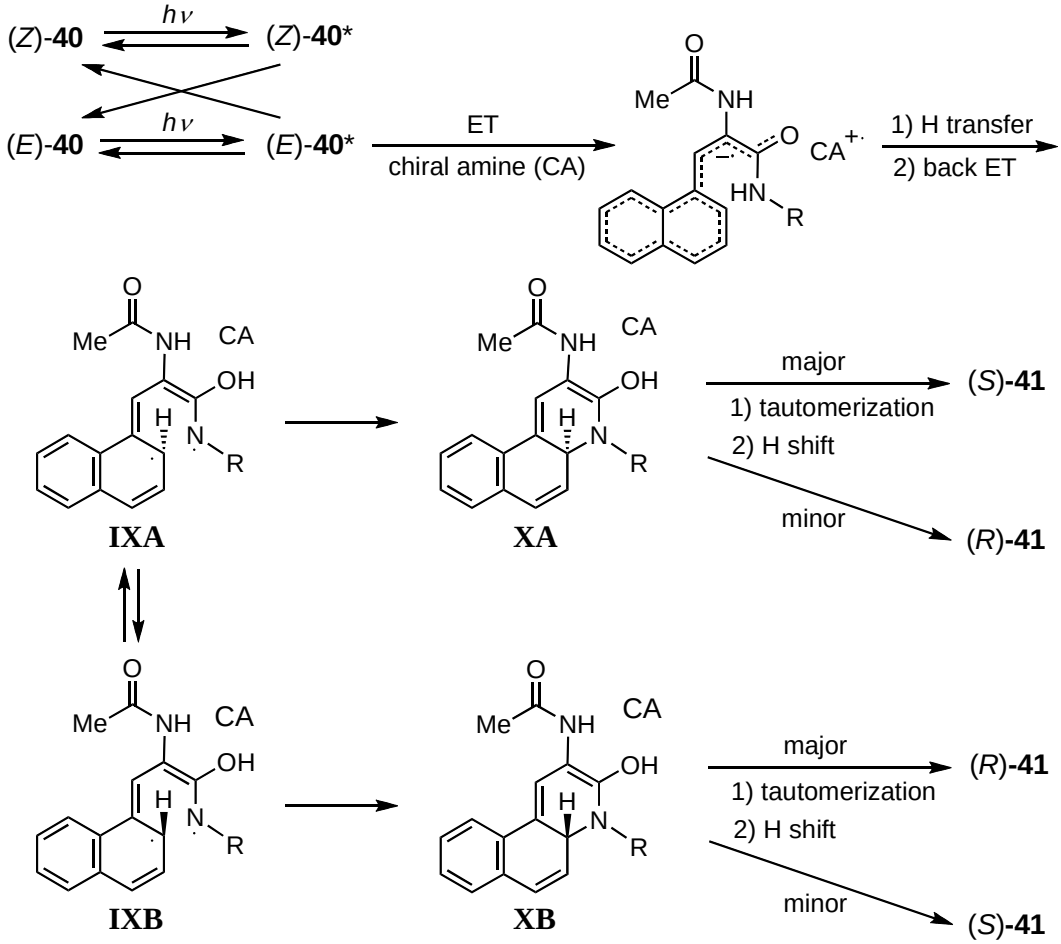

Scheme 25

In addition, in the PET-initiated enantioselective cyclization reactions of (*Z*)-**40**, it is reasonable to assume a pre-equilibrium between the biradical enol intermediates **IXA** and **IXB**, depicted in Scheme 25,

to explain the observed chiral amine, temperature, and substituent effects. Thus, the foregoing hydrogen-bonding interaction is considered to control the pre-equilibrium and assist the tautomerization of the cyclized enol intermediates **XA** and **XB**. The fact that the (*S*)- and (*R*)-enantiomers are produced in excess in the presence of S-NT and S-MPM, respectively, confirms that the former chiral amine is preferentially hydrogen bonded to the biradical enol **IX** (R = Me) in the *si* face and the latter amine to the *re* face (Figure 14).

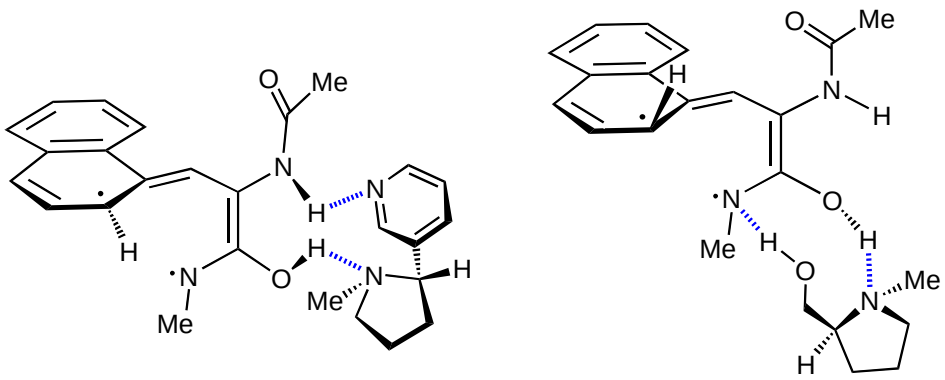

Figure 14. Hydrogen-bonding interactions between the biradical enol **IX** and S-NT or S-MPM

3-3. Chiral auxiliary-substituted (*Z*)-*N*-benzoyl-α-dehydronaphthylalanine alkyl esters and related derivatives[31–33]

In the preceding chapter, we described the selective formation of substituted 4,5-dihydrooxazoles by the PET-initiated cyclization reactions of (*Z*)-*N*-benzoyl-α-dehydroarylalanine alkyl esters. As the 4,5-dihydrooxazole ring possesses two asymmetric carbon atoms in its ring, it was possible to develop a novel PET-initiated asymmetric cyclization reaction of these α-dehydroarylalanine alkyl esters by introducing a chiral auxiliary into the ester moiety.

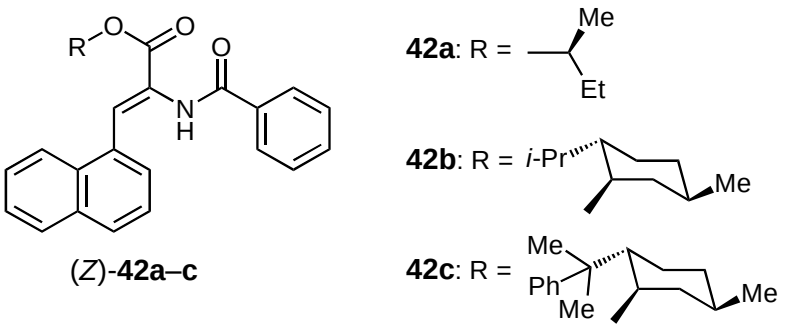

(*Z*)-**42a–c**

42a: R =

42b: R =

42c: R =

Figure 15. Structures of (*Z*)-**42a–c**

To explore the effects of chiral auxiliary, solvent, and temperature on the de for *cis*- and *trans*-4,5-dihydrooxazoles formed in the presence of TEA or 2-(diethylamino)ethanol (DEAE), three types of bulky chiral auxiliary-substituted (*Z*)-*N*-benzoyl-α-dehydro(1-naphthyl)alanine alkyl ester derivatives (*Z*)-**42a**–**c** were designed and synthesized in good yields (Figure 15).

As shown in Scheme 26, irradiation of a nitrogen-saturated methanol solution containing (*Z*)-**42a** and TEA or DEAE at room temperature mainly yielded *trans*-dihydrooxazole-derived diastereomeric mixture [(4*S*,5*R*)-**43a** + (4*R*,5*S*)-**43a**], along with minor amounts of a *cis*-**43a**-derived mixture [(4*R*,5*R*)-**43a** + (4*S*,5*S*)-**43a**]. These four diastereomers were readily isolated, and the successful growth of single crystals of the diastereomer (4*S*,5*S*)-**43d** (Ar = 1-naphthyl, R = *t*-Bu), the structure of which is very similar to that of (4*S*,5*S*)-**43a**, enabled the determination of absolute configurations of the four diastereomers isolated, on the basis of the sign of their CD bands at 220 nm and their ^{1}H NMR spectral and HPLC data (Figure 16).

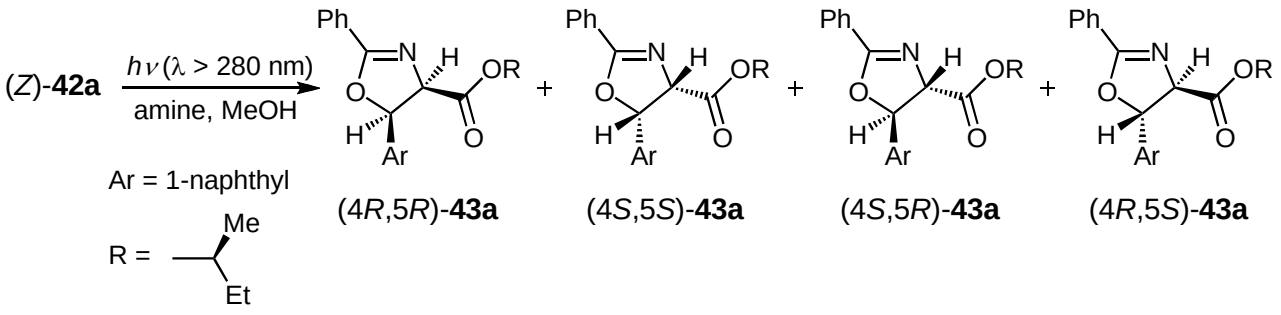

Scheme 26

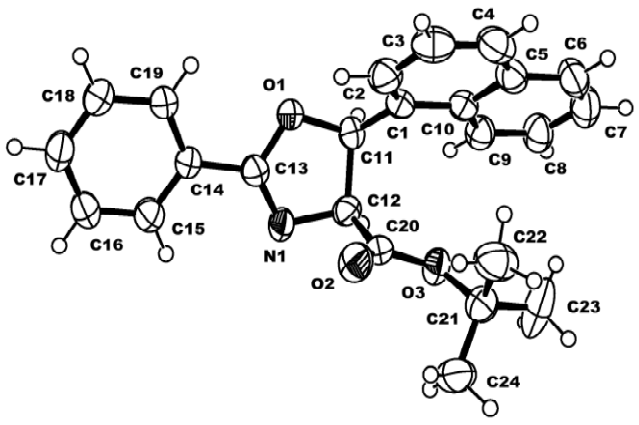

Figure 16. Crystal structure of the diastereomer (4*S*,5*S*)-**43d**

The diastereomer compositions and de values, summarized in Table 13, reveal that the change in solvents from methanol to 1,2-dichloroethane reverses the configuration of the major diastereomer for *cis*-**43a**,**b** without affecting it for *trans*-**43a**,**b**. Additionally, the introduction of a bulky phenylmenthyl auxiliary

results in a great increase in de, especially for *trans*-**43c**, without affecting it for the *cis*- and *trans*-diastereomers formed in these two solvents. These findings suggest that steric and hydrogen-bonding interactions in the π-face selective cyclization process of the (*E*)-**42**-derived radical ion pair intermediate **XI** and a hydrogen shift within the biradical intermediate **XIII** play predominant roles in inducing asymmetry at the 5- and 4-positions of the dihydrooxazole ring, respectively, as depicted in Scheme 27.

Table 13. Effects of substituent, solvent, and tertiary amine on the photoreactivity of **42** and de for *cis*-**43** and *trans*-**43** at room temperature (3 h irradiation)

			Composition and de (%)							
					cis-**43**			*trans*-**43**		
(*Z*)-**42**	Solvent	Amine	(*Z*)-**42**	(*E*)-**42**	(4*R*,5*R*)-**43**	(4*S*,5*S*)-**43**	de	(4*S*,5*R*)-**43**	(4*R*,5*S*)-**43**	de
42a	MeOH	TEA	9.3	21.8	29.3	24.0	10	8.8	6.8	13
42a	$ClCH_2CH_2Cl$	TEA	2.5	3.4	26.2	29.1	5	23.1	15.7	19
42a	MeOH	DEAE	10.2	22.8	8.9	6.2	18	30.7	21.2	18
42a	$ClCH_2CH_2Cl$	DEAE	8.3	18.0	18.3	20.6	6	19.8	15.0	14
42b	MeOH	DEAE	11.0	30.5	19.3	28.9	20	3.4	6.9	34
42b	$ClCH_2CH_2Cl$	DEAE	4.5	9.5	33.7	26.0	13	8.5	17.8	35
42c	MeOH	DEAE	20.2	36.1	4.3	20.2	65	2.8	16.4	71
42c	$ClCH_2CH_2Cl$	DEAE	29.2	29.2	5.0	7.0	17	2.8	26.8	81

Evidence supporting the hydrogen-bonding interactions of DEAE with the (*E*)-**42**-derived reaction intermediates and/or methanol results from the observations that the de's for *cis*-**43** and *trans*-**43** formed in 1,2-dichloroethane are increased (9% → 30% for the former and 22% → 47% for the latter) with decreasing temperature (50 °C → –78 °C), whereas their de values in methanol are abruptly decreased at –78 °C (32% at 50 °C → 0% at –78 °C for the former and 33% → 11% for the latter). Because configurational interconversions between the intermediates **XIIA** and **XIIB** and between the intermediates **XIIIA** and **XIIIB** are unlikely to occur during irradiation, we could estimate the compositions of these intermediates and the rate ratios of Paths A, B, and C on the basis of the four diastereomer compositions (Table 14).

Comparison of the composition of **XIIA** with that of **XIIB** confirms that asymmetric induction for (*Z*)-**42a** and (*Z*)-**42b** in 1,2-dichloroethane is achieved at the stage of hydrogen shift in the biradical intermediate **XIII** while the difference in the radical ion pair **XII**-forming cyclization rates is responsible for asymmetric induction in methanol. Additionally, the finding that the presence of the phenylmenthyl auxiliary in (*Z*)-**42c** greatly enhances the relative composition of **XIIA** in both solvents implies that steric

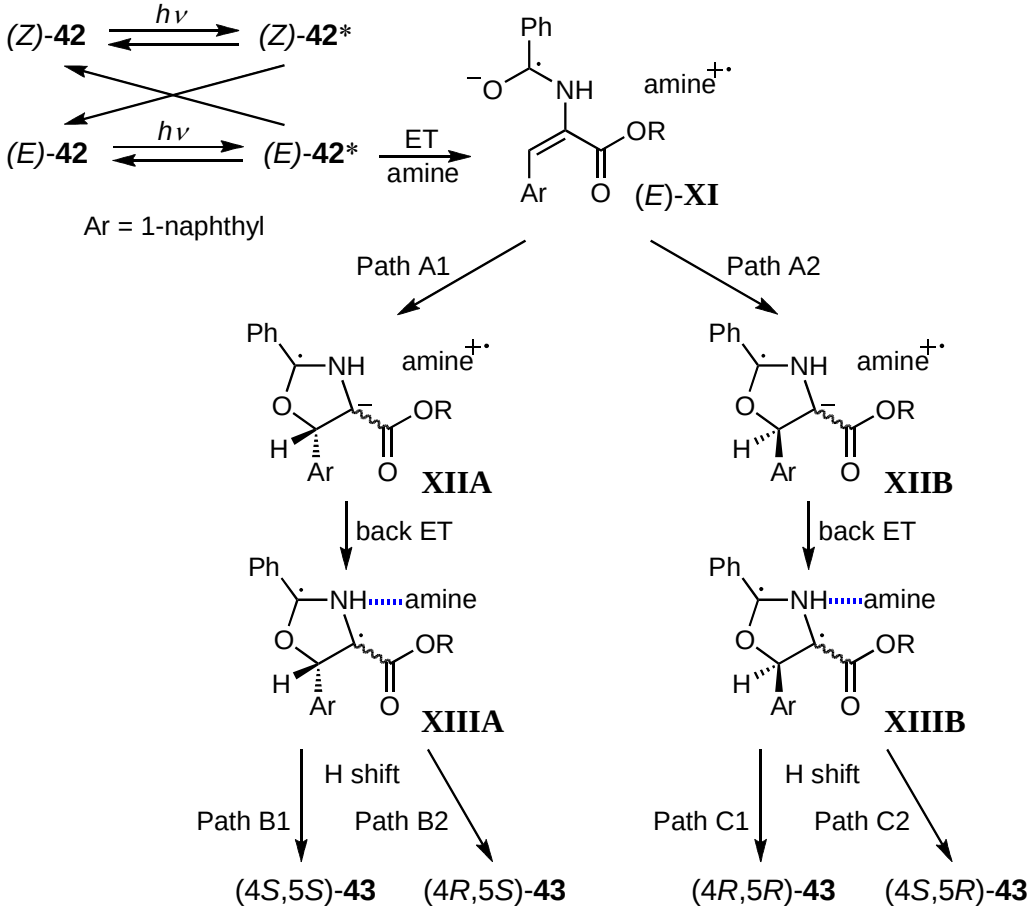

Scheme 27

Table 14. Effects of substituent and solvent on the composition of **XII** and rate ratio (*R*r) of given two competing pathways at room temperature

		Composition of **XII** (%) and *R*r				
(*Z*)-**42**	Solvent	**XIIA**	**XIIB**	*R*r (A1/A2)	*R*r (B1/B2)	*R*r (C1/C2)
42a	MeOH	27.4	39.6	0.7	0.3	0.3
	$ClCH_2CH_2Cl$	35.6	38.1	0.9	1.4	0.9
42b	MeOH	35.8	22.7	1.6	4.2	5.7
	$ClCH_2CH_2Cl$	43.8	42.2	1.0	1.5	4.0
42c	MeOH	36.6	7.1	5.2	1.2	1.5
	$ClCH_2CH_2Cl$	33.8	7.8	4.3	0.3	1.8

repulsion between this bulky chiral auxiliary and the *N*-benzoyl carbonyl oxygen in the radical ion pair (*E*)-**XI** is a dominant factor controlling the relative rate of Path A (Scheme 27). The bulky

phenylmenthyl group is considered to exist preferentially in the *re* face of (*E*)-**XI**, leading to a cycloaddition reaction in the *si* face of this intermediate.

As already demonstrated, the replacement of the alkoxycarbonyl group in *N*-benzoyl-α-dehydro(1-naphthyl)alanine alkyl esters by the *N′*,*N′*-disubstituted aminocarbonyl completely suppressed the TEA-catalyzed isomerization of *cis*-4,5-dihydrooxazole derivatives formed, although the amidation of the ester moiety lowered the photoreactivity. Furthermore, the increased steric bulk of the alkoxy carbonyl group enhanced selectivity for the *cis*-dihydrooxazole isomer. Thus, it is predicted that the introduction of a sterically congested chiral auxiliary into the naphthylalaninamide nitrogen enables the selective formation of this *cis*-isomer; hence, a more detailed analysis of the diastereoselective PET-initiated cyclization reactions of (*Z*)-**44a**–**g** is required (Figure 17).

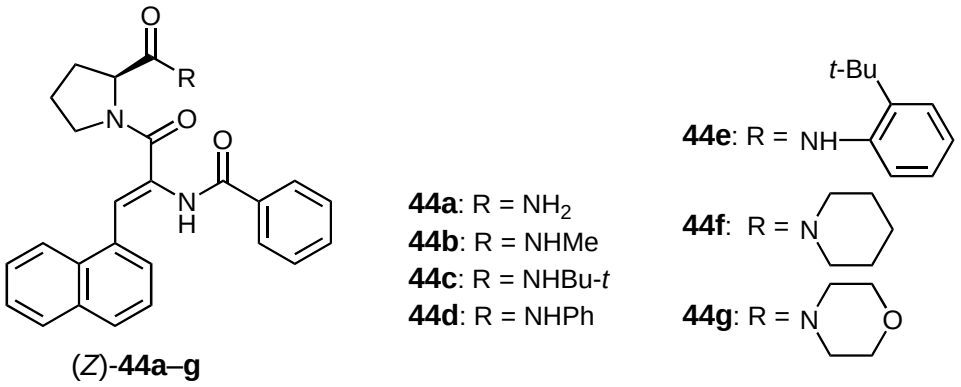

Figure 17. Structures of (*Z*)-**44a**–**g**

Irradiation of a nitrogen-saturated methanol solution containing (*Z*)-**44a** and TEA selectively gave the corresponding *cis*-dihydrooxazole-derived diastereomers (4*S*,5*S*)-**45a** and (4*R*,5*R*)-**45a**, as predicted (Scheme 28).

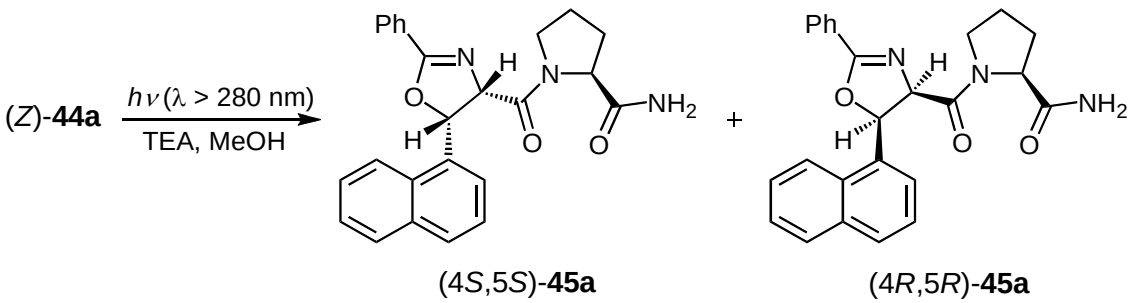

Scheme 28

The absolute configurations and compositions of these two diastereomers and the de's were determined on the basis of their CD and ^{1}H NMR spectral data and summarized in Table 15.

When the solvent was changed from 1,2-dichloroethane to methanol, the configuration of the major diastereomer formed was reversed to afford (4*R*,5*R*)-**45** in excess in all systems. Intermolecular hydrogen-bonding interactions between this protic solvent molecule and a key intermediate, probably a radical ion pair intermediate, and/or intramolecular hydrogen-bonding interactions within this intermediate are considered to exert a significant effect on the intermediate configuration. As can be

Table 15. Effects of substituent and solvent on the conversion of **44** and de for (4*S*,5*S*)-**45** or (4*R*,5*R*)-**45** at room temperature

(*Z*)-**44**	Solvent	Conversion (%)	Composition (%)		de (%)
			(4*S*,5*S*)-**45**	(4*R*,5*R*)-**45**	
44a	$ClCH_2CH_2Cl$	22	15.4	7.0	38
44b	$ClCH_2CH_2Cl$	22	16.3	5.7	48
44c	$ClCH_2CH_2Cl$	44	37.6	5.9	73
44d	$ClCH_2CH_2Cl$	15	12.3	2.7	64
44e	$ClCH_2CH_2Cl$	29	26.4	2.3	84
44f	$ClCH_2CH_2Cl$	63	38.0	25.0	21
44g	$ClCH_2CH_2Cl$	60	37.3	22.5	25
44a	MeOH	28	11.0	17.3	22
44b	MeOH	22	7.3	14.5	33
44c	MeOH	34	9.7	24.3	43
44d	MeOH	28	8.9	18.9	36
44e	MeOH	34	14.0	20.1	18
44f	MeOH	89	25.8	62.9	42
44g	MeOH	87	25.0	62.4	43

inferred from Scheme 29, no formation of *trans*-**45** suggests that the hydrogen shift in the biradical **XVI** occurs stereoselectively; hence, de for the *cis*-isomer is determined in the cyclization of the radical ion pair (*E*)-**XIV** to **XV**. It is likely that hydrogen-bonding and steric interactions in (*E*)-**XIV** play decisive roles in controlling stereochemistry of the π-face selective attack of the *N*-benzoyl carbonyl oxygen.

Analysis of the effects of the aprotic and protic solvents on the magnitude of de for *cis*-**45g**, summarized in Table 16, shows that de for (4*R*,5*R*)-**45g** is enhanced with decreasing polarity of protic solvents (de in: MeOH < *i*-PrOH < *t*-BuOH), and this de value has a marked tendency to increase as the polarity of aprotic solvents is lowered (de in: CH_2ClCH_2Cl < CH_2Cl_2 < $CHCl_3$), although the configuration of the major diastereomer formed in 1,2-dichloroethane is different from that obtained in dichloromethane and chloroform. Because the (4*R*,5*R*)-diastereomer is formed as a major photoproduct in methanol, these

findings suggest that in addition to the electrostatic interaction in the initially formed radical ion pair intermediate (*E*)-**XIV**, a charge-transfer interaction operates between the radical anion in this intermediate and dichloromethane or chloroform. Additional stabilization of (*E*)-**XIV** through these electrostatic and hydrogen-bonding interactions is also reflected in a large increase in the photoreactivity of the starting (*Z*)-**44g**.

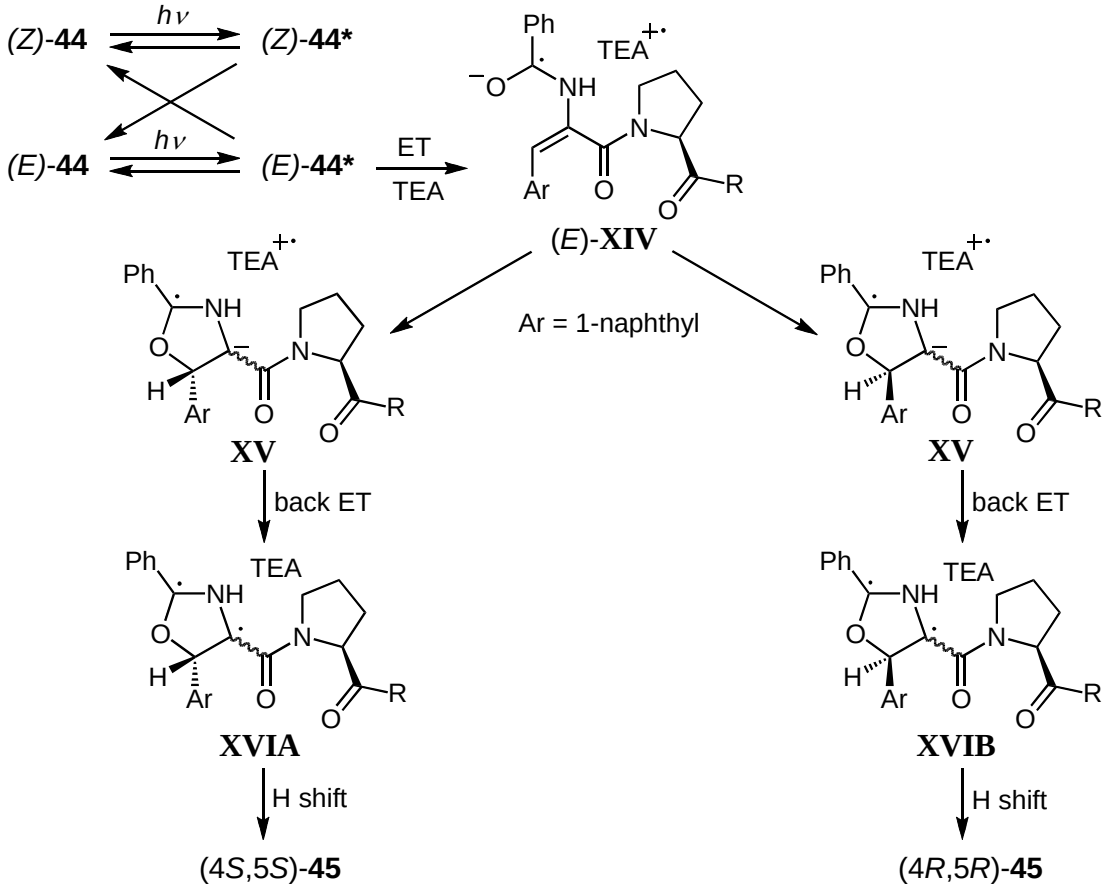

Scheme 29

Table 16. Composition for (4*S*,5*S*)-**45g** and (4*R*,5*R*)-**45g**, de for the major diastereomer, and conversion of **44g**, estimated in each solvent containing TEA at room temperature

Solvent	Conversion (%)	Composition (%)		de (%)
		(4*S*,5*S*)-**45g**	(4*R*,5*R*)-**45g**	
MeOH	87	25.0	62.4	43
i-PrOH	39	4.2	34.5	78
t-BuOH	24	1.5	22.8	88
$ClCH_2CH_2Cl$	60	37.3	22.5	25
CH_2Cl_2	100	23.0	77.0	54
$CHCl_3$	100	9.1	90.9	82

3-4. (*Z*)-*N*-Benzoyl-α-dehydronaphthylalanine *tert*-butyl esters[33–35]

In the preceding section, we showed that asymmetric induction in the PET-initiated cyclizations of chiral auxiliary-substituted α-dehydroamino acid derivatives was achieved at the stages of intramolecular cycloaddition in the radical ion pair intermediate and hydrogen shift in the biradical intermediate. At the former stage, the steric bulk of chiral auxiliaries is a significant factor controlling the magnitude of de, while at the latter stage, the hydrogen-bonding interaction between the biradical intermediate and aliphatic amine is a major factor governing this magnitude. Thus, the use of chiral amines such as S-PM and S-MPM (Figure 13) was predicted to bring about an asymmetric photocyclization of (*Z*)-*N*-benzoyl-α-dehydronaphthylalanine *tert*-butyl esters (*Z*)-**46a**,**b** (Figure 18).

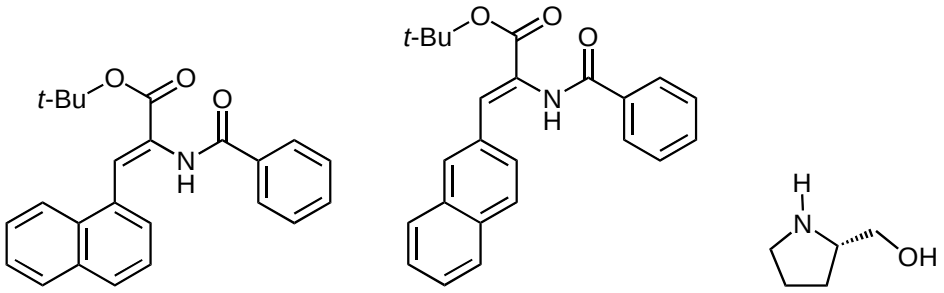

(*Z*)-**46a** (*Z*)-**46b** S-PM

Figure 18. Structures of (*Z*)-**46a**,**b** and S-PM

The PET-initiated cyclization reactions of (*Z*)-**46** quantitatively proceeded in the presence of S-MPM to produce four types of the 4,5-dihydrooxazole enantiomers (Scheme 30). The absolute configuration of these enantiomers and the ee were determined according to the procedure described in the preceding section (Table 17). Additionally, the relative compositions of the biradical intermediates **XIIIA** and **XIIIB** (R = *t*-Bu in Scheme 27) and the rate ratios of Paths A, B, and C were estimated from the relative compositions of (4*S*,5*S*)-**47**, (4*R*,5*S*)-**47**, (4*R*,5*R*)-**47**, and (4*S*,5*R*)-**47** and collected in Table 18.

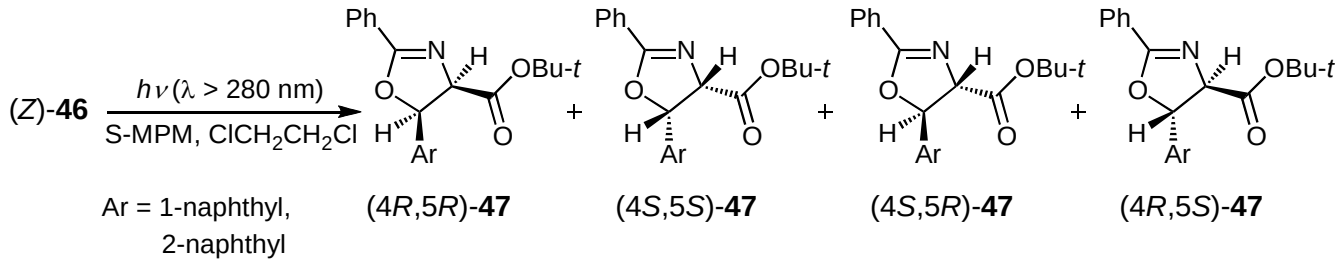

Scheme 30

Table 17. Effects of substituent and chiral amine on the conversion of **46** and ee for *cis*-**47** and *trans*-**47** in 1,2-dichloroethane at room temperature

(*Z*)-**46**	Chiral amine	Conversion (%)	Composition and ee (%)					
			cis-**47**			*trans*-**47**		
			(4*R*,5*R*)-**47**	(4*S*,5*S*)-**47**	ee	(4*S*,5*R*)-**47**	(4*R*,5*S*)-**47**	ee
46a	S-MPM	100	36.6	24.8	19	12.9	25.7	33
46b	S-MPM	100	26.6	12.5	36	24.4	36.5	20
46a	S-PM	97	13.0	23.6	29	37.1	26.3	17

Table 18. Effects of substituent and chiral amine on the composition of **XIII** and rate ratio (*R*r) of given two competing pathways at room temperature

(*Z*)-**46**	Chiral amine	Composition of **XIII** (%) and *R*r				
		XIIIA	**XIIIB**	*R*r (A1/A2)	*R*r (B1/B2)	*R*r (C1/C2)
46a	S-MPM	50.5	49.5	1.0	1.0	2.8
46b	S-MPM	49.0	51.0	1.0	0.3	1.1
46a	S-PM	49.9	50.1	1.0	0.9	0.4

Clearly, the rate ratio *R*r (A1/A2) for the cyclization process of the radical ion pair (*E*)-**XI** is unity, irrespective of the starting α-dehydronaphthylalanine *tert*-butyl ester and chiral amine (Table 18). Thus, the finding that the replacement of the 1-naphthyl group by the 2-naphthyl enhances ee for *cis*-**47**, with a decrease in ee for *trans*-**47** may be explained by the different steric effects of these naphthyl groups on the hydrogen shift in the *re* and *si* faces of the intermediate **XIII** (Table 17). Further inspection of the data in Table 17 shows that when S-PM is used instead of S-MPM, the configuration of major enantiomers for *cis*-**47** and *trans*-**47** is reversed. Participation of the hydrogen-bonded biradical **XIII** in the key step of asymmetric induction suggests that S-MPM assists the hydrogen shift on the *si* face through hydrogen bonds formed between the N–Me nitrogen in this chiral amine and N–H hydrogen in **XIII** and between the O–H hydrogen and ester carbonyl oxygen in this intermediate, as depicted in Figure 19. In contrast, S-PM partially blocks the *si* face through similar hydrogen-bonding interactions to promote a hydrogen shift in the *re* face (Figure 19).

On the other hand, irradiation of a nitrogen-saturated 1,2-dichloroethane solution containing (*Z*)-*N*-benzoyl-α-dehydro(1-naphthyl)alanine *N′*-arylamides (*Z*)-**48a**,**b** and S-MPM almost quantitatively afforded the corresponding four 4,5-dihydrooxazole enantiomers (4*R*,5*R*)-**49**, (4*S*,5*S*)-**49**, (4*S*,5*R*)-**49**, and

(4*R*,5*S*)-**49** (Scheme 31).

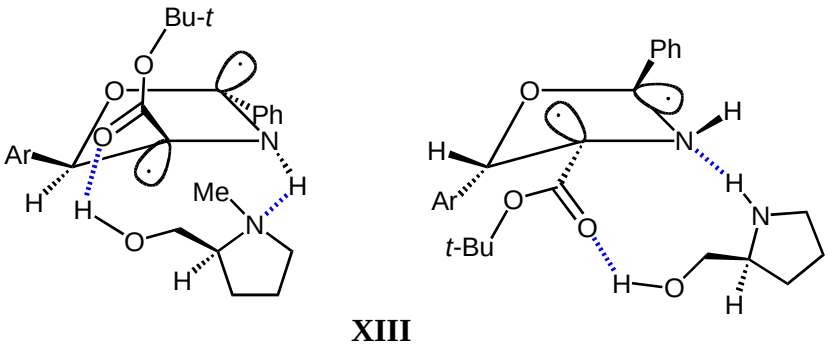

XIII

Figure 19. Hydrogen-bonding interactions of the biradical intermediate **XIII** with S-MPM and S-PM

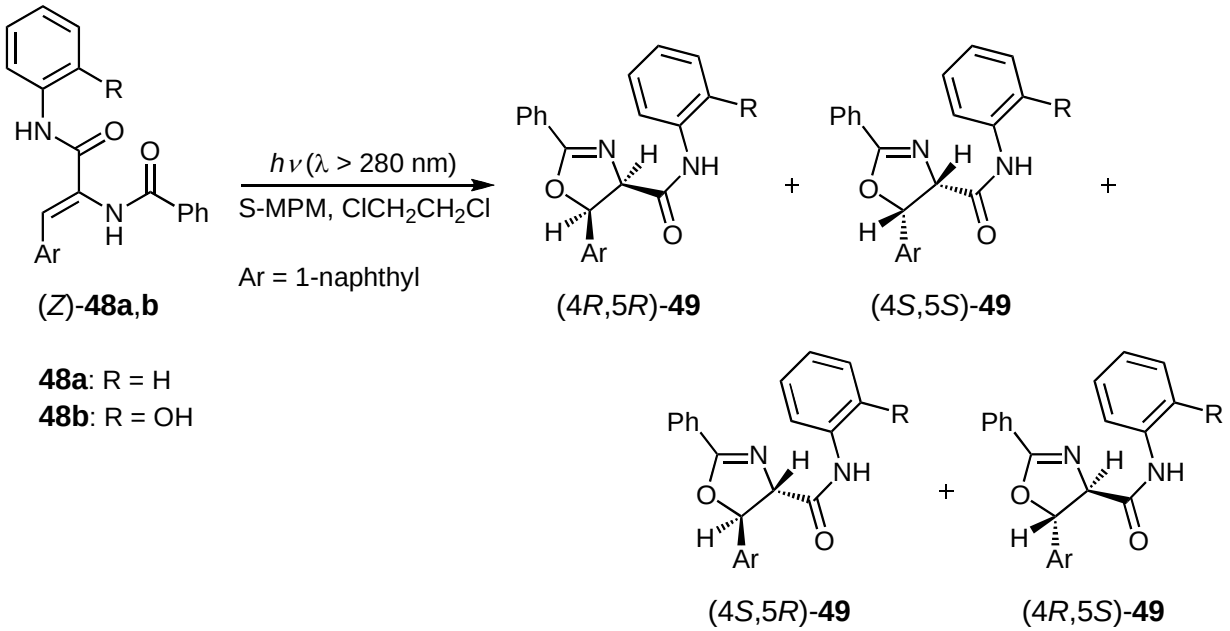

Scheme 31

Analysis of the compositions of these enantiomers, collected in Table 19, establishes that the introduction of a phenolic hydroxy group into (*Z*)-**48a** dramatically lowers ee's for (4*S*,5*S*)-**49a** and (4*R*,5*S*)-**49a**. This finding indicates the negligible participation of a hydrogen-bonding interaction between the aforementioned biradical intermediate and S-MPM in the hydrogen shift within this intermediate. It is likely that intramolecular hydrogen bonding between the N–H nitrogen and phenolic O–H hydrogen in the **48b**-derived biradical intermediate, depicted in Figure 20, inhibits the formation of intermolecular hydrogen bonding between S-MPM and this intermediate and increases the relative rate of the hydrogen shift forming the *trans*-dihydrooxazole isomer. Therefore, the findings described above provide additional evidence for the intervention of a hydrogen-bonded biradical intermediate in the enantioselective photocyclization process of *N*-benzoyl-α-dehydro(1-naphthyl)alanine *tert*-butyl esters.

Table 19. Substituent effects on the ee for *cis*-**49** and *trans*-**49**, obtained in the presence of S-MPM at room temperature

(*Z*)-**48**	Conversion (%)	Composition and ee (%)					
		cis-**49**			*trans*-**49**		
		(4*R*,5*R*)-**49**	(4*S*,5*S*)-**49**	ee	(4*R*,5*S*)-**49**	(4*S*,5*R*)-**49**	ee
48a	100	37.5	53.0	17	6.6	2.9	39
48b	100	28.1	28.7	1	21.6	21.6	0

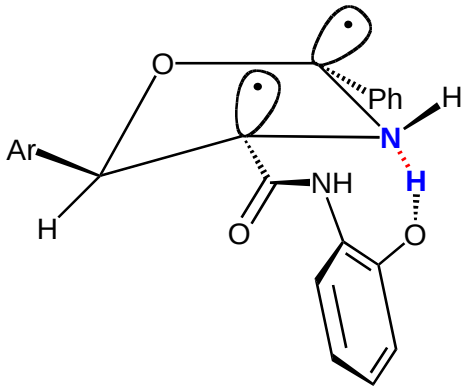

Figure 20. Intramolecular hydrogen-bonding interaction in the **48b**-derived biradical intermediate

4. CONCLUSION

In this review we highlighted not only PET-initiated cyclization reactions of various (*Z*)-*N*-acyl-α-dehydroarylalanine *N*′-alkylamides, (*Z*)-*N*-acyl-α-dehydroarylalanine alkyl esters, and 1,2,4-triazole-substituted (*Z*)-α-dehydroarylalaninamides but also asymmetric transformations of these α-dehydroarylalanine derivatives.

The intramolecular and intermolecular PET reactions of α-dehydroarylalanine *N*′-alkylamides in methanol cleanly and efficiently proceeded to mainly produce variously substituted 3,4-dihydroquinolinones, along with minor amounts of isoquinolines and 4,5-dihydrooxazoles, the compositions of which varied depending on the steric bulk of the *N*-acyl and *N*′-alkyl groups. The replacement of the *N*′-amide bond in *N*-aroyl-α-dehydroarylalaninamides by the ester bond exerted a dramatic effect on the product distribution to cause a selective formation of 4,5-dihydrooxazole derivatives. Inspection of this structural effect on the product distribution and composition revealed that (*Z*)- and (*E*)-α-dehydroarylalanine isomers in the excited state serve as the precursors of substituted isoquinolines and dihydroquinolinones/dihydrooxazoles, respectively. When the 1,2,4-triazol-4-yl group was introduced instead of the acylamino group, the PET reactions of the triazole-substituted

derivatives afforded substituted quinolinones and dihydroquinolinones without forming any other products, and the composition ratio of these two heterocyclic compounds greatly varied depending on the properties of solvents and substituents examined. Mechanistic analysis of the aforementioned three types of PET-initiated cyclization reactions revealed that the stability of the α-dehydroarylalanine radical anion/aliphatic amine radical cation pair intermediate plays a key role in controlling the distribution and composition of the photocyclization reaction products.

In addition, through the detailed analysis of the effects of chiral auxiliary, chiral amine, aryl and alkyl substituents, protic and aprotic solvents, and temperature on the PET-initiated asymmetric photocyclization reactions enabling the construction of chiral 3,4-dihydroquinolinone and 4,5-dihydrooxazole rings, we were led to propose the following asymmetry-inducing processes: (1) the tautomerization process of the (*E*)-*N*-acyl-α-dehydroarylalaninamide-derived hydrogen-bonded enol intermediates and (2) the cyclization process of the (*E*)-*N*-acyl-α-dehydroarylalanine alkyl ester-derived radical anion intermediates and the hydrogen shift process of the hydrogen-bonded biradical intermediates, which served as the precursors of the corresponding 4,5-dihydrooxazole derivatives. Furthermore, we could show that the magnitude of de or ee for these asymmetric photocyclization reactions was mainly controlled by the steric and electronic effects of the chiral auxiliary or chiral amine on the asymmetry-inducing processes described above.

ACKNOWLEDGEMENTS

Our study described in this review was partially supported by a 'High-Tech Research Project' and a 'Scientific Frontier Research Project' from the Ministry of Education, Culture, Sports, Science and Technology in Japan.

REFERENCES

1. a) K. Mizuno, N. Ichinose, and Y. Yoshimi, *J. Photochem. Photobiol., C*, 2000, **1**, 167; b) N. Hoffman, 'CRC Handbook of Organic Photochemistry and Photobiology,' 2nd ed., ed. by W. M. Horspool and F. Lenci, CRC Press, Florida, 2004, pp. **34**-1–**34**-20; c) N. J. Turro, V. Ramamurthy, and J. C. Scaiano, 'Modern Molecular Photochemistry of Organic Molecules,' University Science Books, California, 2010.
2. a) 'Synthetic Organic Photochemistry,' ed. by W. M. Horspool, Plenum, New York, 1984; b) 'Handbook of Photochemistry and Photobiology,' Vol. 2, ed. by H. S. Nalwa, American Scientific Publishers, California, 2003; c) 'Synthetic Organic Photochemistry,' ed. by A. G. Griesbeck and J. Mattay, Marcel Dekker, New York, 2005; d) A. G. Griesbeck, N. Hoffmann, and K. Warzecha, *Acc. Chem. Res.*, 2007, **40**, 128; e) M. Kitamura and K. Narasaka, *Bull. Chem. Soc. Jpn.*, 2008, **81**, 539; f)

D. W. Cho, U. C. Yoon, and P. S. Mariano, *Acc. Chem. Res.*, 2011, **44**, 204.

3. S. Hunt, 'Chemistry and Biochemistry of the Amino Acids,' ed. by G. C. Barrett, Chapman and Hall, New York, 1985, pp. 392–393.
4. K. Kubo, Y. Ishii, T. Sakurai, and M. Makino, *Tetrahedron Lett.*, 1998, **39**, 4083.
5. T. Motohashi, K. Maekawa, K. Kubo, T. Igarashi, and T. Sakurai, *Heterocycles*, 2002, **57**, 269.
6. K. Oshimi, K. Kubo, A. Kawasaki, K. Maekawa, T. Igarashi, and T. Sakurai, *Tetrahedron Lett.*, 2002, **43**, 3291.
7. A. Kawasaki, K. Maekawa, K. Kubo, T. Igarashi, and T. Sakurai, *Tetrahedron*, 2004, **60**, 9517.
8. T. Sakurai, K. Miyoshi, M. Obitsu, and H. Inoue, *Ber. Bunsenges. Phys. Chem.*, 1996, **100**, 46.
9. a) K. Noda, Y. Shimohigashi, and N. Izumiya, 'The Peptides–Analysis, Synthesis, Biology,' Vol. 5 (Part B), ed. by E. Gross and J. Meienhofer, Academic Press, New York, 1983, pp. 305–308; b) Y. S. Rao and R. Filler, *Synthesis*, 1975, 749; c) B. Rzeszotarska, J. Karolak-Wojciechowska, M. A. Broda, Z. Galdecki, B. Trzezwinska, and A. E. Koziol, *Int. J. Peptide Protein Res.*, 1994, **44**, 313.
10. a) W. I. Awad and A. E. A. G. Allah, *J. Org. Chem.*, 1960, **25**, 1242; b) K. Lempert, J. Nyitrai, P. Sohar, and K. Zauer, *Tetrahedron Lett.*, 1964, **5**, 2679; c) A. Mustafa, W. Asker, A. H. Harhash, T. M. S. Abdin, and E. M. Zayed, *Liebigs Ann. Chem.*, 1968, **714**, 146; d) C. W. Bird and J. D. Twibell, *J. Chem. Soc. (C)*, 1971, 3155; e) G. Simig, K. Lempert, and J. Tamas, *Tetrahedron*, 1973, **29**, 3571; f) U. Schoellkopf, H.-H. Hausberg, M. Segal, U. Reiter, I. Hoppe, W. Saenger, and K. Lindner, *Liebigs Ann. Chem.*, 1981, 439; g) J. K. Rasmussen, S. M. Heilmann, L. R. Krepski, H. K. Smith II, A. R. Katritzky, and K. Sakizadeh, *J. Polym. Sci. Polym. Chem. Ed.*, 1986, **24**, 2739; h) A. Jain and A. K. Mukerjee, *J. Indian Chem. Soc.*, 1990, **67**, 973; i) S.-S. Homami and A. K. Mukerjee, *Indian J. Chem. Sect. B*, 1991, **30**, 288; j) H. M. Hassan, O. M. O. Habib, and Y. M. Darwish, *Rev. Roum. Chim.*, 1992, **37**, 1029; k) M. Mazik, R. Boese, and R. Sustmann, *Liebigs Ann.*, 1996, 1665; l) S. Grivas and P. Schuisky, *Heterocycles*, 1998, **48**, 1575; m) K. Nalepa, G. Zednikova, J. Marek, and Z. Travnicek, *Monatsh. Chem.*, 1999, **130**, 471; n) P. M. Shafi and T. D. Sobha, *Indian J. Chem. Sect. B*, 1999, **38**, 378.
11. K. Maekawa, T. Igarashi, K. Kubo, and T. Sakurai, *Tetrahedron*, 2001, **57**, 5515.
12. K. Maekawa, A. Shinozuka, M. Naito, T. Igarashi, and T. Sakurai, *Tetrahedron*, 2004, **60**, 10293.
13. K. Maekawa, K. Fujita, K. Iizuka, T. Igarashi, and T. Sakurai, *Heterocycles*, 2005, **65**, 117.
14. a) G. R. Lenz, *Synthesis*, 1978, 489; b) S. Naruto and O. Yonemitsu, *Chem. Pharm. Bull.*, 1980, **28**, 900; c) I. Ninomiya, C. Hashimoto, T. Kiguchi, and T. Naito, *J. Chem. Soc., Perkin Trans. 1*, 1985, 941; d) K. Jones, M. Thompson, and C. Wright, *J. Chem. Soc., Chem. Commun.*, 1986, 115; e) G. P. Johnson and B. A. Marples, *J. Chem. Soc., Perkin Trans. 1*, 1988, 3399; f) A. L. Beck, M. Mascal, C. J. Moody, and W. J. Coates, *J. Chem. Soc., Perkin Trans. 1*, 1992, 813; g) R. Rezaie, J. B. Bremner,

G. K. Blanch, B. W. Skelton, and A. H. White, *Heterocycles*, 1995, **41**, 959; h) B. E. Ali, K. Okuro, G. Vasapollo, and H. Alper, *J. Am. Chem. Soc.*, 1996, **118**, 4264; i) T. Nishio, H. Asai, and T. Miyazaki, *Helv. Chim. Acta*, 2000, **83**, 1475; j) H. Zhao, A. Thurkauf, J. Braun, R. Brodbeck, and A. Kieltyka, *Bioorg. Med. Chem. Lett.*, 2000, **10**, 2119; k) C. Jia, D. Piao, T. Kitamura, and Y. Fujiwara, *J. Org. Chem.*, 2000, **65**, 7516; l) J.-Y. Legros, G. Primault, and J.-C. Fiaud, *Tetrahedron*, 2001, **57**, 2507; m) K. S. Feldman, T. D. Cutarelli, and R. D. Florio, *J. Org. Chem.*, 2002, **67**, 8528; n) W. R. Bowman, A. J. Fletcher, and G. B. S. Potts, *J. Chem. Soc., Perkin Trans. 1*, 2002, 2747.

15. a) I. Ninomiya and T. Naito, *Heterocycles*, 1981, **15**, 1433; b) I. Ninomiya, C. Hashimoto, T. Kiguchi, and T. Naito, *J. Chem. Soc., Perkin Trans. 1*, 1983, 2967; c) T. Naito, Y. Tada, and I. Ninomiya, *Heterocycles*, 1984, **22**, 237.
16. K. Maekawa, A. Tomoda, T. Igarashi, and T. Sakurai, *Heterocycles*, 2008, **75**, 2959.
17. K. Maekawa, A. Tomoda, T. Igarashi, and T. Sakurai, *Heterocycles*, 2009, **77**, 739.
18. Y. Yazawa, M. Suzuki, T. Igarashi, and T. Sakurai, *Heterocycles*, 2010, **80**, 199.
19. a) A. M. Dave, K. N. Bhatt, N. K. Undavia, and P. B. Trivedi, *J. Indian Chem. Soc*., 1988, **65**, 294; b) A. A. Afify, S. EI-Nagdy, M. A. Sayed, and I. Mohey, *Indian J. Chem., Sect. B*, 1988, **27**, 920; c) V. Kepe, F. Pozgan, A. Golobic, S. Polanc, and M. Kocevar, *J. Chem. Soc., Perkin Trans. 1*, 1998, 2813; d) O. H. Hishmat, N. M. Fawzy, D. S. Farrag, and A. S. Abd EI-AII, *Rev. Roum. Chim*., 1999, **44**, 161; e) C. T. Brain, J. M. Paul, Y. Loong, and P. J. Oakley, *Tetrahedron Lett*., 1999, **40**, 3275; f) S. Polanc, *Targets in Heterocyclic Systems*, 1999, **3**, 33; g) F. A. A. EI-Mariah, H. A. Saad, H. A. Allimony, and R. M. Abdel-Rahman, *Indian J. Chem., Sect. B*, 2000, **39**, 36; h) A. V. Naidu and M. A. Dave, *Asian J. Chem*., 2000, **12**, 679; i) A. V. Naidu and M. A. Dave, *Asian J. Chem*., 2000, **12**, 914; j) N. C. Desai, D. Dave, M. D. Shah, and G. D. Vyas, *Indian J. Chem., Sect. B*, 2000, **39**, 277; k) E. C. Lawson, B. E. Maryanoff, and W. J. Hoekstra, *Tetrahedron Lett*., 2000, **41**, 4533; l) M. D. Shah, N. C. Desai, K. K. Awasthi, and A. K. Saxena, *Indian J. Chem., Sect. B*, 2001, **40**, 201; m) F. Pozgan, S. Polanc, and M. Kocebar, *Heterocycles*, 2001, **54**, 1011; n) S. D. Trivedi, H. T. Kubawat, and H. H. Parekh, *J. Indian Chem. Soc*., 2002, **79**, 282.
20. a) R. A. Abramovitch, J. M. Beckert, H. H. Gibson, Jr., A. Belcher, G. Hundt, T. Sierra, S. Olivella, W. T. Pennington, and A. Sole, *J. Org. Chem*., 2001, **66**, 1242; b) M. J. Paterson, M. A. Robb, L. Blancafort, and A. D. DeBellis, *J. Am. Chem. Soc*., 2004, **126**, 2912.
21. a) O. Meth-Cohn, *Heterocycles*, 1993, **35**, 539; b) C. W. Holzapfel and C. Dwyer, *Heterocycles*, 1998, **48**, 215; c) K. Y. Lee and J. N. Kim, *Bull. Korean Chem. Soc*., 2002, **23**, 939; d) B. Joseph, F. Darro, A. Behard, B. Lesur, F. Collignon, C. Decaestecker, A. Frydman, G. Guillaumet, and R. Kiss, *J. Med. Chem*., 2002, **45**, 2543; e) D. V. Kadnikov and R. C. Larock, *J. Organomet. Chem*., 2003, **687**, 425; f) M. Hadjeri, C. Beney, and A. Boumendjel, *Curr. Org. Chem*., 2003, **7**, 679; g) S. K.

Chattopadhyay, R. Dey, and S. Biswas, *Synthesis*, 2005, 403; h) Q. Li, K. W. Woods, W. Wang, N.-H. Lin, A. Claiborne, W.-Z. Gu, J. Cohen, V. S. Stoll, C. Hutchins, D. Frost, S. H. Rosenberg, and H. L. Sham, *Bioorg. Med. Chem. Lett.*, 2005, **15**, 2033; i) M. Asahara, M. Ohtsutsumi, M. Tamura, N. Nishiwaki, and M. Ariga, *Bull. Chem. Soc. Jpn.*, 2005, **78**, 2235; j) R. Bernini, S. Cacchi, G. Fabrizi, and A. Sferrazza, *Heterocycles*, 2006, **69**, 99; k) R. Bernini, S. Cacchi, I. De Salve, and G. Fabrizi, *Synlett.*, 2006, 2947.

22. T. Horaguchi, N. Hosokawa, K. Tanemura, and T. Suzuki, *J. Heterocycl. Chem.*, 2002, **39**, 61.
23. K. Maekawa, T. Sasaki, K. Kubo, T. Igarashi, and T. Sakurai, *Tetrahedron Lett.*, 2004, **45**, 3663.
24. K. Maekawa, N. Hishikawa, K. Kubo, T. Igarashi, and T. Sakurai, *Tetrahedron*, 2007, **63**, 11267.
25. Y. Sato, A. Yoshida, T. Igarashi, and T. Sakurai, *Heterocycles*, 2010, **81**, 997.
26. a) L. E. Overman, S. Tsuboi, and S. Angle, *J. Org. Chem.*, 1979, **44**, 2323; b) K. Burger, E. Huber, W. Schöntag, and R. Ottlinger, *J. Chem. Soc., Chem. Commun.*, 1983, 945; c) C. A. Ibarra, J. A. Cereceda, P. Ortiz, A. Vicente, and M. L. Quiroga, *Tetrahedron Lett.*, 1985, **26**, 243; d) D. Roberto and H. Alper, *J. Chem. Soc., Chem. Commun.*, 1987, 212; e) F. Minozzi and P. Venturello, *J. Chem. Soc., Chem. Commun.*, 1987, 1255; f) A. Hassner, A. S. Amarasekara, and D. Andisik, *J. Org. Chem.*, 1988, **53**, 27; g) P. Wipf and C. P. Miller, *Tetrahedron Lett.*, 1992, **33**, 907; h) J. Einsiedel, C. Schoerner, and P. Gmeiner, *Tetrahedron*, 2003, **59**, 3403.
27. K. Maekawa, T. Igarashi, K. Kubo, and T. Sakurai, *Heterocycles*, 2002, **57**, 1591.
28. K. Maekawa, K. Kubo, T. Igarashi, and T. Sakurai, *Tetrahedron*, 2004, **60**, 1183.
29. K. Maekawa, K. Kubo, T. Igarashi, and T. Sakurai, *Tetrahedron*, 2005, **61**, 11211.
30. K. Maekawa, T. Tanami, T. Igarashi, and T. Sakurai, *Heterocycles*, 2011, **83**, 2255.
31. Y. Sasaki, K. Maekawa, H. Watanabe, T. Matsumoto, K. Kubo, T. Igarashi, and T. Sakurai, *Tetrahedron Lett.*, 2007, **48**, 4765.
32. Y. Sato, Y. Haruyama, T. Igarashi, and T. Sakurai, *Heterocycles*, 2010, **82**, 603.
33. Y. Sasaki, H. Watanabe, T. Igarashi, and T. Sakurai, *Heterocycles*, 2011, **83**, 1329.
34. H. Watanabe, K. Maekawa, T. Igarashi, and T. Sakurai, *Heterocycles*, 2007, **74**, 149.
35. H. Yadai, Y. Sato, T. Igarashi, and T. Sakurai, *Heterocycles*, 2012, **84**, 737.

Tadamitsu Sakurai was born in Matsushima, Japan in 1947. He received his B. Sc (1970) from Kanagawa University and his Ph.D. (1976) from Osaka City University under the direction of Prof. Shigeru Oae. Then, he spent two years (1976–1978) in the group of Prof. Marion H. O'Leary at the University of Wisconsin in Madison, USA and then one year (1978 –1979) in the group of Prof. George L. Kenyon at the University of California in San Francisco as a research associate. In 1979, he joined Prof. Hiroyasu Inoue's group at Kanagawa University as an Assistant Professor. In 1994, he was promoted to Full Professor and began his independent research career. His research interests include the development of new types of photochemical reaction systems and their application to photofunctional materials.

Tetsutaro Igarashi was born in Yokohama, Japan in 1949. He received his B. Sc (1973) from Kanto Gakuin University. In 1968, he was appointed as a chemical engineering technician at Kanagawa University, where he became a senior technician in 1985. His research interests are mainly in the area of carbohydrate chemistry and organic photochemistry.